NASA Contractor Report 186014

A Preliminary Look at an Optimal Multivariable Design for Propulsion-Only Flight Control of Jet-Transport Aircraft

Christopher P. Azzano

Contract SA 258-21
April 1992

National Aeronautics and
Space Administration

NASA Contractor Report 186014

A Preliminary Look at an Optimal Multivariable Design for Propulsion-Only Flight Control of Jet-Transport Aircraft

Christopher P. Azzano
San Jose State University Foundation
San Jose, California

Prepared for
NASA Dryden Flight Research Facility
Edwards, California
Under Contract SA 258-21

1992

National Aeronautics and
Space Administration

Dryden Flight Research Facility
Edwards, California 93523-0273

CONTENTS

LIST OF TABLES

LIST OF FIGURES

ABSTRACT

Control of a large jet-transport aircraft without the use of conventional control surfaces was investigated. Engine commands were used to attempt to recreate the forces and moments typically provided by the elevator, ailerons, and rudder. Necessary conditions for aircraft controllability (disturbability) were developed pertaining to aircraft configuration such as the number of engines and engine placement. An optimal linear quadratic regulator controller was developed for the Boeing 707-720, in particular, for regulation of its natural dynamic modes. The design employed a method of assigning relative weights to the natural modes, for example, phugoid and dutch roll, for a more intuitive selection of the cost function. A prototype pilot command interface was then integrated into the loop based on pseudorate command of both pitch and roll. Closed-loop dynamics were evaluated first with a batch linear simulation and then with a real-time high fidelity piloted simulation. The NASA research pilots assisted in evaluation of closed-loop handling qualities for typical cruise and landing tasks. Recommendations for improvement on this preliminary study of optimal propulsion-only flight control are provided in this report.

INTRODUCTION

Recent interest in propulsion-enhanced aircraft control has stemmed from the recognition of considerable performance increments by integrating the propulsion and flight control systems. Development of these systems can provide the capability of performing a wide range of flight control tasks from enhanced-maneuverability of a high-performance fighter aircraft to outright control of large jet-transport aircraft. The latter capability has gained particular attention recently because of the in-flight hydraulic failures on United Airlines flight 232, a McDonnell Douglas DC-10, and Japan Airlines flight 123, a Boeing 747. In each instance, the mishap aircraft exhibited some degree of controllability with adroit throttle manipulation but was destroyed during an unsuccessful landing attempt. Furthermore, since other sources of conventional control loss could result from mechanical failure or fly-by-wire malfunction, it becomes clear that an alternate mode of control using the engines as the only actuators is desirable.

This control mode is most critical for large jet-transport aircraft because of their poor open-loop handling characteristics and the lack of capability for in-flight passenger egress. The existence of a high fidelity, piloted simulation for the Boeing 707-720 on site also contributed to the decision to make jet transports the focus of this preliminary investigation. The problem has become known as propulsion-only flight control.

Technical assistance from Stanford University, Department of Aeronautics and Astrophysics, Stanford, California, is gratefully acknowledged. In addition, a special acknowledgement goes to the San Jose State University Foundation, San Jose, California, for funding the optimal control portion of this propulsion-only research effort.

NOMENCLATURE

A, B	system matrices
bank limit	upper and lower bound on bank angle command limiter
C	controllability matrix
C_{ℓ_β}	nondimensional yaw-roll coupling derivative
c.g.	center of gravity
dc	direct current (steady state)
FCS	flight control system
fpm	ft/min
fps	ft/sec

h	altitude
I_{xx}, I_{yy}, I_{zz}	moments of inertia about x, y, and z axes respectively
I_{xz}	product of inertia referred to x and z axes
Im	Imaginary
J	cost function to be minimized
K	gain matrix
LQR	linear quadratic regulator
M	Mach number
MAC	mean aerodynamic chord
MIMO	multiinput/multioutput
NASA	National Aeronautics and Space Administration
n	number of state variables
PIO	pilot-induced oscillation
POFCS	propulsion-only flight control system
p	roll rate
p_{stick}	lateral stick gain
pitch limit	upper and lower bound on pitch command limiter
Q	state weighting matrix
q	pitch rate
q_{stick}	longitudinal stick gain
R	control weighting matrix
Re	Real
r	yaw rate
S	solution to Ricatti equation
SISO	single-input/single-output
T	thrust
T_s	piloted simulation sample period
t	time
u	control input vector; aircraft velocity component along x-axis
V	modal matrix; total aircraft velocity
v	aircraft velocity component along y-axis
w	aircraft velocity component along z-axis
x	state vector
$x_{hydro.cutoff}$	values of state variable at the time hydraulics are lost
z	complex variable (discrete time)
$\frac{d}{dt}$	derivative with respect to time
$\int() dt$	integration over time
α	angle of attack
β	sideslip angle
δ_{stick}	stick command

δ_T	perturbed engine throttle commands
ζ	damping coefficient
θ	pitch angle
σ	standard deviation
ϕ	bank angle
ψ	heading angle
ω_n	natural frequency

Superscripts:

T	transpose
-1	inverse
$\cdot$	derivative with respect to time

Subscripts:

c	command
d	desired
il	inboard left engine
ir	inboard right engine
lat	lateral
lng	longitudinal
ol	outboard left engine
or	outboard right engine
r	regulator feedback
ss	steady state
T	thrust
$\_$	transformed variable

DESIGN GOALS

Ideally, a propulsion-only flight control system (POFCS) would provide acceptable handling qualities in the event of any type of catastrophic flight control system (FCS) malfunction. Unfortunately, many factors can prevent the realization of ideal performance. The physics of the problem demonstrates that feasibility of a POFCS requires satisfying two fundamental requirements. First, the engine time-constants must be smaller than the time-constants of the dynamic modes being controlled. Second, an aircraft with engines as the only actuators must demonstrate mathematical controllability (disturbability) for each of the dynamic modes being controlled.

Both requirements are configuration-dependent, and their satisfaction is determined by the airframe and power-plant designers. Although many modern high-bypass turbofan engines have spool-up/spool-down times of roughly 8 to 10 seconds, the natural frequencies of the dynamic modes for aircraft using these engines are proportionally lower. Thus, the first criterion will present less of a problem than the second. Satisfaction of the second criterion depends most strongly on the number of engines, their location with respect to the aircraft center of gravity (c.g.), and their orientation with respect to the aircraft body axes. Just how these factors relate to propulsion-only controllability is discussed.

Assuming the two conditions are satisfied, the engines will have the capability to recreate the forces and moments, normally provided by conventional control surfaces, necessary for flightpath control. Then, the problem becomes using this capability to achieve the following design goals:

1. Acceptable regulation of natural aircraft dynamic modes that contribute to undesirable handling qualities, for example, phugoid and dutch roll modes;
2. Development of a pilot interface that blends conventional throttle and stick commands into a single engine-power command by way of an appropriate control hierarchy; and
3. Acceptable handling qualities and pilot workload in cruise, approach-to-landing, and missed-approach tasks.

A preliminary attempt to reach these goals uses a linear quadratic regulator (LQR) design with pseudorate command pilot interface. The specifics of such a process are discussed below.

OPTIMAL PROPULSION-ONLY CONTROL DESIGN

As an alternative to the classical successive loop closure design technique, this study employed a linear quadratic algorithm to design optimal multiinput/multioutput (MIMO) gains for the regulator portion of the controller. The LQR method was selected for the following reasons:

1. The LQR is optimal with respect to a specified cost function.
2. The LQR algorithm takes advantage of the complex couplings within a multiinput/multioutput system.
3. The LQR technique guarantees a stable controller in the absence of modeling uncertainties.
4. The LQR design allows intuitive assignment of relative regulator effort to each of the natural modes of motion through transformation of the linearized equations of motion to modal coordinates, a property that is particularly useful with the very limited control authority provided by jet engines.
5. The LQR algorithm provides a controller robust to parameter uncertainties with proper selection of a "loose" cost function.

Drawbacks of LQR design include a more complex gain and feedback loop structure, in comparison to the classical single-input/single-output (SISO) intuition of relative gain size and its effect on performance, particularly stability. Practice and design iteration, however, should lead to an overall better controller than successive loop closure. It is important to remember that performance benefits in a severely degraded system such as a POFCS may be barely discernible.

Overview of the Linear Quadratic Regulator Design Method

The LQR algorithm provides a time-varying regulator of the form

$$u = -Kx \tag{1}$$

that minimizes the cost function

$$J = 0.5 \int (x^T Q x + u^T R u)\, dt \tag{2}$$

subject to the linear equations of motion

$$\dot{x} = Ax + Bu \tag{3}$$

as constraints. The weighting matrices Q and R are typically assigned only diagonal positive nonzero elements, providing a cost function that is the sum of weighted squares of the state variables x and control inputs u. The optimal gain matrix is computed as

$$K = R^{-1}B^{T}S \tag{4}$$

where S is the solution to the Ricatti equation

$$\dot{S} = SA + A^{T}S - SBR^{-1}B^{T}S + Q \tag{5}$$

Over the history of regulation, the time-varying gains approach zero as the error in the state-vector approaches zero, and the terminal condition is achieved (figure 1). Typically, the constant steady-state portion of the time-varying gain is used for the entire trajectory, simplifying controller implementation. The resulting control law is

$$u = -K_{ss}x \tag{6}$$

See reference 1 for a thorough derivation.

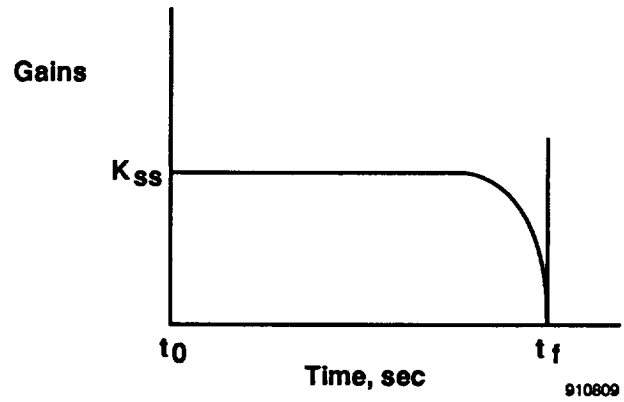

Figure 1. Optimal time-varying linear quadratic regulator gains.

Conditions Necessary for Controllability

Mathematical controllability (disturbability) of a linear system may be evaluated by defining controllability matrix C as

$$C = [B\ AB\ A^{2}B\ \ldots\ A^{n}B] \tag{7}$$

where A and B are the system matrices, and n is the number of state variables. A system is then said to be controllable, that is, all the dynamic modes can be affected by the existing actuators to achieve any desired final state if the matrix C has rank n (reference 2). For a real physical system, it is rare that C will have other than full rank, so a more discriminating criterion for controllability is required. The condition number of the controllability matrix, which is, the ratio of the largest eigenvalue of C to the smallest, provides a measure of controllability, a larger value indicating a less-controllable system. In other words, the largest eigenvalue represents a mode that is most strongly influenced by one or more of the actuators, and the smallest eigenvalue represents that mode which is least affected.

The condition number of the controllability matrix for an aircraft under engine-only control is determined primarily by airframe configuration (A) and the number of engines and their location (B). Although a rigorous derivation is excluded here, necessary conditions for controllability of all aircraft dynamics modes with a POFCS include

1. Longitudinal dynamics. To control pitch and velocity independently, and thus the short-period and phugoid modes, it is necessary to have two engine thrust lines with different vertical displacements from the c.g.
2. Lateral-directional dynamics. To control yaw (which couples through C_{ℓ_β} to roll), and thus the roll, dutch roll and spiral modes, it is necessary to have at least one engine thrust line with a nonzero lateral displacement from the c.g.
3. Longitudinal dynamics independent of lateral. To control pitch and velocity independently without affecting yaw, it is necessary to have thrust lines with different vertical displacements from the c.g., and no combined effective lateral displacement, i.e., on the lateral plane of symmetry or displaced on both sides of the lateral plane of symmetry allowing yawing moment cancellation.
4. Lateral dynamics independent of longitudinal. To control yaw without affecting either pitch or velocity, it is necessary to have a thrust line with nonzero lateral displacement from the c.g., another thrust line anywhere to control velocity, and one with a different vertical displacement to equalize pitching moments.

These conditions assume that engines out of the lateral plane of symmetry have thrust lines nearly aligned with the longitudinal axis, and thus have little or no capacity to provide direct rolling moment. Such alignment is typical of jet transports. These conditions are satisfied by any of the existing three-engine (DC-10, L1011, or 727) or four-engine (747, 707, and DC-8) jet transports. Two-engine configurations such as the DC-9, 767, 757, or 737 may exhibit additional performance degradation and may be impossible to fly without additional means of actuation, such as electronic stabilator trim.

Modal Regulator Design Using the Linear Quadratic Regulator Method

An alternate formulation of the LQR problem involves transforming the equations of motion to a more desirable set of coordinates than those defining the original state variables. Weighting matrices are then assigned to the transformed state vector, and the resulting gains are optimal for the revised problem. A simple transformation back to the original coordinates provides LQR gains for use in the feedback loop.

A natural choice for an alternate set of coordinates is one in which the transformed state-variables are defined in modal coordinates. This choice is achieved by performing the transformation,

$$x = V\underline{x} \tag{8}$$

from the original coordinates x to an augmented set $\underline{x}$ via the matrix V whose columns contain the eigenvectors of the system matrix A. The transformed equations then become

$$\dot{\underline{x}} = V^{-1}AV\underline{x} + V^{-1}Bu \tag{9}$$

The cost function is defined by way of weighting matrices $\underline{Q}$ and the original R. The advantage here is that LQR weights may be assigned directly to aircraft dynamic modes, such as the dutch roll or spiral, providing a very intuitive cost function definition. The results in figures 2 and 3 clearly illustrate the utility of working in modal coordinates.

The set of gains $\underline{K}$ provided in this transformed LQR design is easily converted for use with the original state variables according to

$$K = \underline{K}V^{-1} \tag{10}$$

such that the actual feedback control law becomes

$$u = -\underline{K}V^{-1}x \tag{11}$$

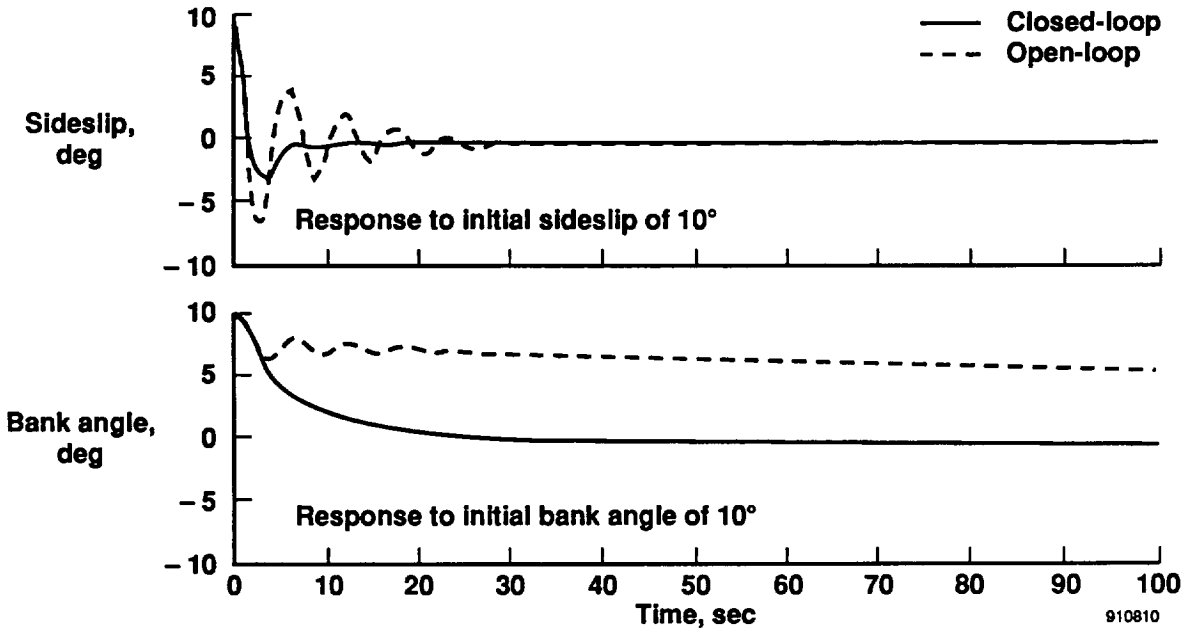

Figure 2. Utility of linear quadratic regulator design with modal criteria, spiral/dutch roll tradeoff, where dutch roll weight >> spiral weight.

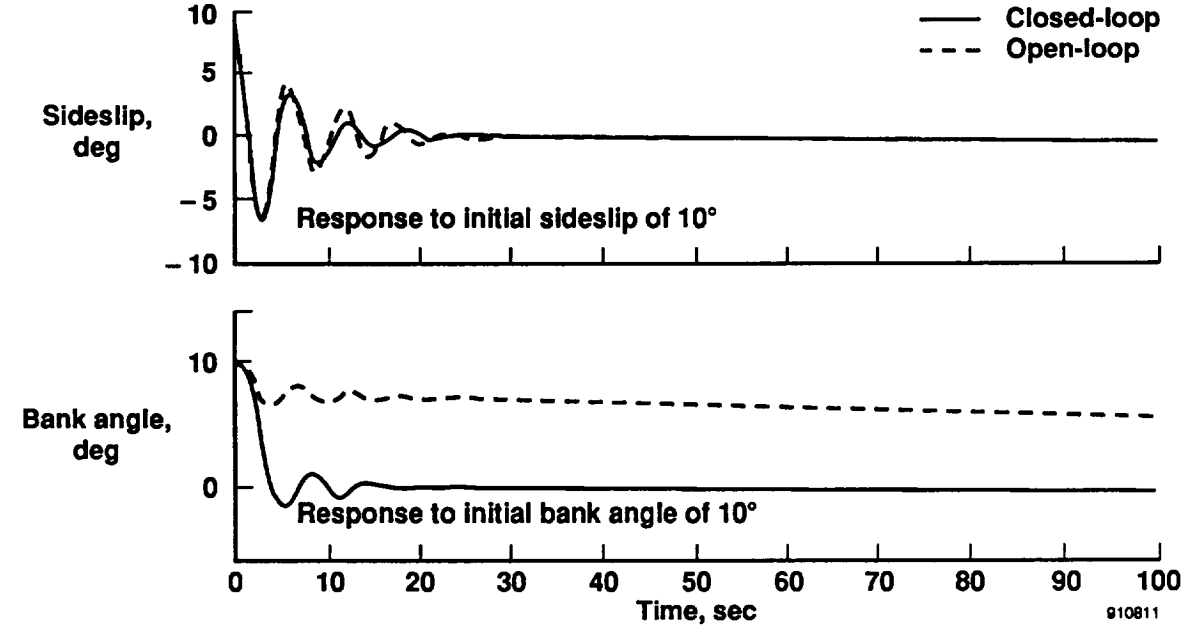

Figure 3. Utility of linear quadratic regulator design with modal criteria, spiral/dutch roll tradeoff, where spiral weight >> dutch roll weight.

It is important to note two factors. First, depending on the algorithm, the eigenvectors contained in V may not always be ordered consistently, and care must be taken that the weights assigned in $\underline{Q}$ correspond to the desired modal coordinates. Second, assigning LQR weights is often easier if the equations of motion are first normalized such that weights of the same order of magnitude have the same influence on the cost function. For example, working with pounds and radians in the same cost function will generally result in weights varying by five orders of magnitude since variables will typically reach values in the thousands of pounds and no more than a few hundredths of radians. A better formulation might nondimensionalize by kilopounds and centiradians.

Pilot Command Interface

With the regulator loop designed, the more difficult task of developing an interface for pilot commands must be addressed. Development is complicated by the multiple performance tradeoffs and handling qualities requirements, several of which include

1. providing sufficient control authority and bandwidth to the pilot, thereby minimizing pilot-induced oscillation (PIO) tendencies due to engine response time;
2. developing an interface that will not wash out pilot commands;
3. providing handling qualities as close as possible to the "healthy" aircraft; for example, longitudinal stick should exchange potential for kinetic energy; throttles should control total energy; and lateral stick should command roll rate; and
4. making optimal use of limited engine thrust to perform required control tasks.

Typical methods of injecting commands into the loop are illustrated in figures 4 and 5 (reference 3). Each implementation requires inversion of either the plant or loop DC-gain matrix. Unfortunately, neither of these matrices is invertible for the three- or four-engine configurations. The simple physical reason for this limitation is the inability to control, for example, sideslip angle independent of roll rate or velocity independent of angle of attack (α), with the limited control authority available. Note that controllability does not require inversion of either DC-gain matrix.

The simple solution employed in this analysis involves translation of a pilot command directly into a single state-variable command. This method minimizes the possibility of injecting conflicting commands when attempting to achieve a particular response. The only conflict remaining is that zero commands for all but one longitudinal and one lateral state variable may prevent achievement of the desired response in minimum time.

In an aircraft with conventional handling qualities, pitch rate is typically commanded with longitudinal stick and roll rate with lateral stick. The problem with using these two variables for the command interface is that the system becomes incapable of holding a pitch attitude or bank angle. It may be that handling qualities are so degraded by engine response time that it is preferable for the stick to command pitch and bank angles. An alternative is to use a *pseudorate* command that integrates stick position over time to determine a desired final pitch and bank attitude command. The implementation used in this analysis is depicted in figures 6 and 7. This pseudorate command implementation uses the general form illustrated in figure 4.

Note that the integrators are described in the z-plane which is necessary for implementation on the digital piloted simulator. The limiters on both interfaces are to prevent engines from being saturated by pilot commands, ensuring that regulation of dynamic modes is maintained at all times. Maximum stick deflection performance with these limiters is adequate. The switch in the lateral-directional interface is to provide a wings leveling tendency when the commanded bank angle is below a certain value, and the lateral stick displacement is zero.

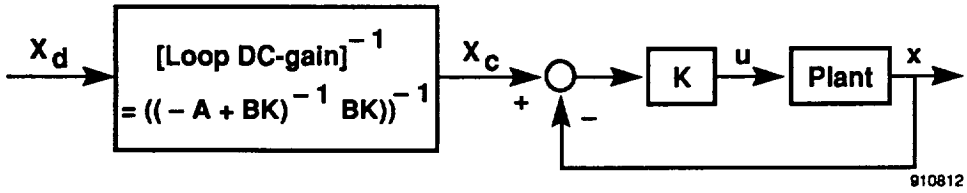

Figure 4. Direct command injection scheme.

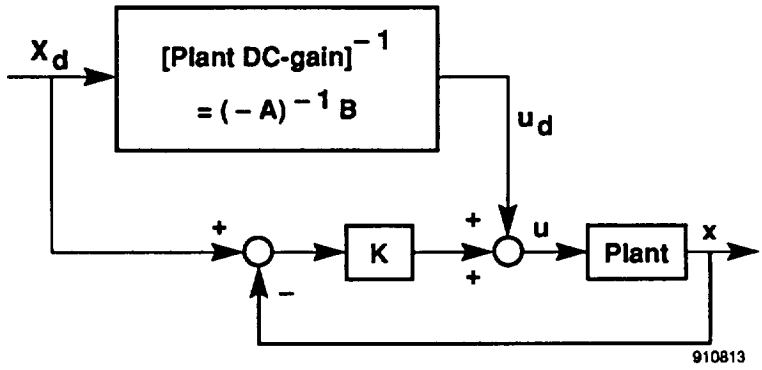

Figure 5. Combined direct and feed-forward injection scheme.

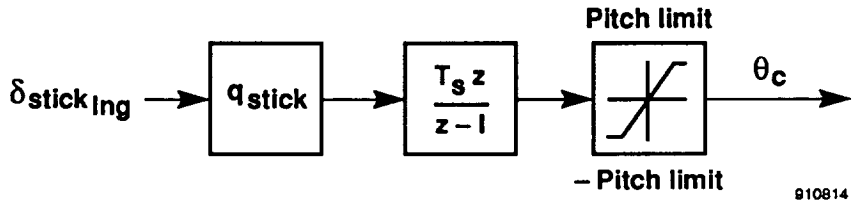

Figure 6. Longitudinal pilot command interface.

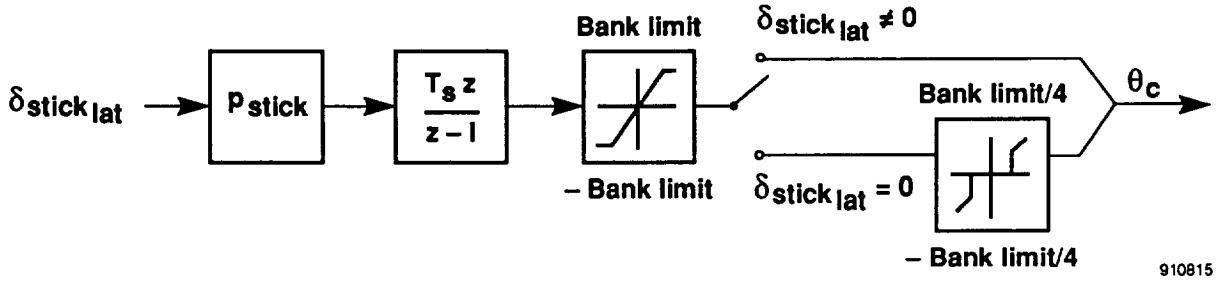

Figure 7. Lateral-directional pilot command interface.

LINEAR ANALYSIS OF THE BOEING 707-720

The modal regulator design using the LQR method was developed and implemented for the Boeing 707-720 (figure 8). A linear analysis was performed before the control design to determine the controllability and open-loop dynamic characteristics. Iteration to a reasonable closed-loop controller then made use of a simple linearized model taken about a wings-level, steady-state, flight condition. Finally, the controller was implemented on the high fidelity nonlinear piloted simulation at NASA Dryden Flight Research Facility (NASA Dryden), and further iterations arrived at a closed-loop system with acceptable handling qualities.

Linear State-Space Model

A linear model obtained from the high fidelity simulation provided longitudinal and lateral-directional state-space equations of motion for the B-720 aircraft under propulsion-only control. Values in the B matrix were the result of steady-state perturbations in thrust and, hence, included no engine dynamics. Since a controller designed with a model assuming instantaneous engine response would clearly lead to an unstable regulator, an appropriate engine model was inferred from thrust transients. The complete model integrated both aircraft and engine dynamics with engine thrust and its time derivative as additional states.

Aircraft Longitudinal and Lateral-Directional Equations of Motion

A brief review of the history of in-flight emergencies revealed that transport pilots were typically satisfied to land with the flaps up if it was suspected that lowering them might induce degraded control. Gear position had only minor effect on closed-loop dynamics. Design at a nominal approach configuration was considered most critical, so the aircraft configuration and flight condition were selected as follows:

altitude	4,000 ft
calibrated airspeed	175 kn
flight condition	straight and level
gross weight	160,000 lb
inertias	
I_{xx}	2,350,000 slug-ft^2
I_{xz}	0 slug-ft^2
I_{yy}	3,440,000 slug-ft^2
I_{zz}	5,715,000 slug-ft^2
c.g.	20.85% MAC
flaps	up
landing gear	up

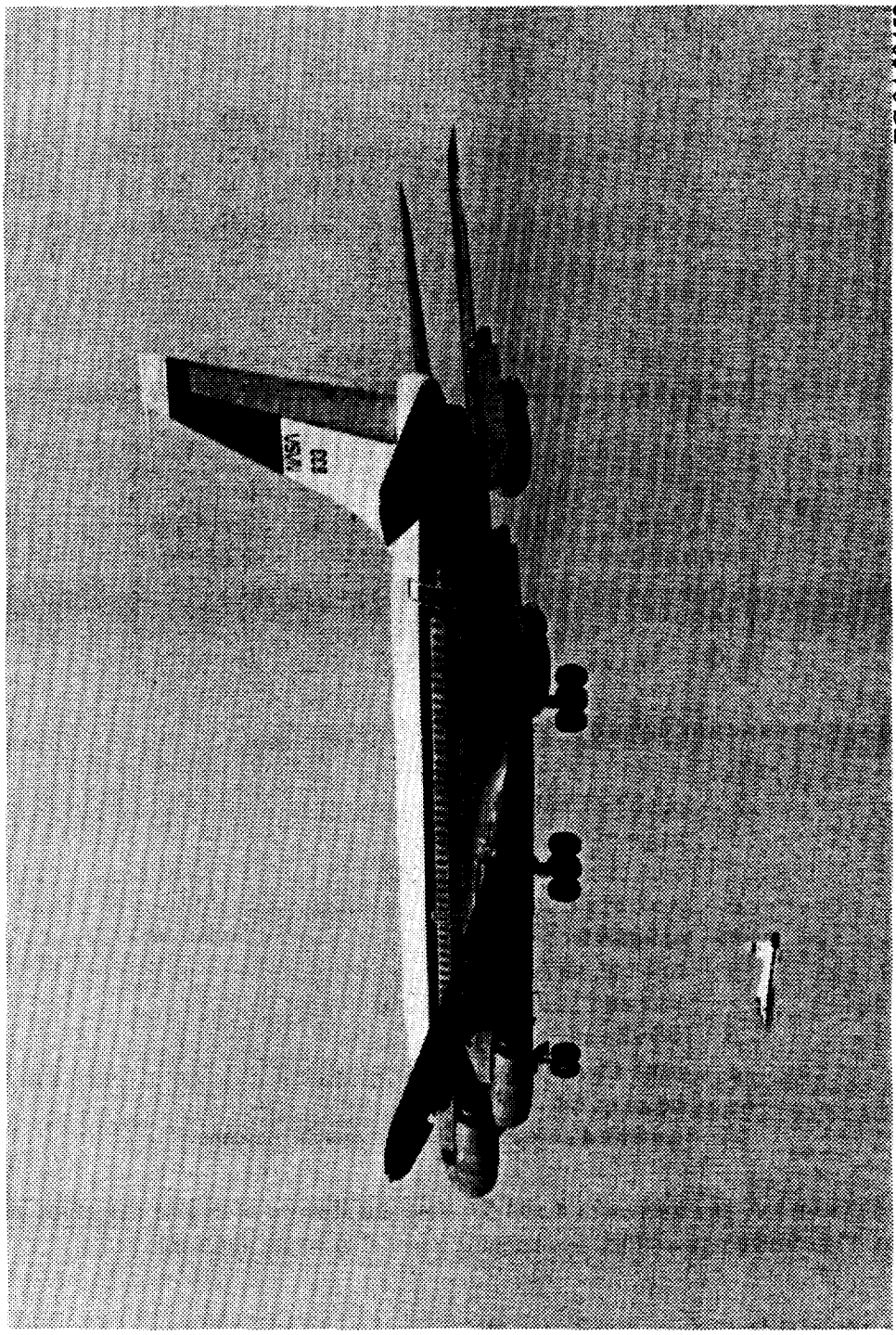

EC 84 28452

Figure 8. Boeing 707-720.

The result was the following model with state-vector $x = \{q\ \alpha\ V\ \theta\ h; p\ r\ \beta\ \phi\ \psi\}^T$ and control vector $u = \{\delta_{Tol}\ \delta_{Til}\ \delta_{Tir}\ \delta_{Tor}\}^T$ defining linearized equations of motion in the form of equation (3):

$$A = \begin{bmatrix} -0.89 & -0.98 & 0.00011 & 0 & 0 & & & & & \\ 1 & -0.79 & -0.00065 & 0 & 0 & & & & & \\ 0 & 13 & -0.012 & -32 & 0.00006 & & & & & \\ 1 & 0 & 0 & 0 & 0 & & & & & \\ 0 & -312 & 0 & 312 & 0 & & & & & \\ & & & & & -0.99 & 0.55 & -3.0 & 0 & 0 \\ & & & & & -0.053 & -0.21 & 0.76 & 0.0021 & 0 \\ & & --- & & & 0.11 & -0.98 & -0.11 & 0.10 & 0 \\ & & & & & 1 & 0.11 & 0 & 0 & 0 \\ & & & & & 0 & 1.01 & 0 & 0 & 0 \end{bmatrix}$$

$$B = \begin{bmatrix} 0.000051 & 0.00012 & 0.00012 & 0.000051 \\ -0.000009 & -0.000009 & -0.000009 & -0.000009 \\ 0.020 & 0.020 & 0.020 & 0.020 \\ 0 & 0 & 0 & 0 \\ 0 & 0 & 0 & 0 \\ 0.000068 & 0.000040 & -0.000040 & -0.000068 \\ 0.00080 & 0.00047 & -0.00047 & -0.00080 \\ 0 & 0 & 0 & 0 \\ 0 & 0 & 0 & 0 \\ 0 & 0 & 0 & 0 \end{bmatrix}$$

where the perturbed state variables are defined as follows:

q	pitch rate, rad/sec
α	angle of attack, rad
V	total aircraft velocity, ft/sec
θ	pitch angle, rad
h	altitude, ft
p	roll rate, rad/sec
r	yaw rate, rad/sec
β	sideslip angle, rad
ϕ	bank angle, rad
ψ	heading, rad
δ_T	perturbed engine throttle commands, percent

For a more detailed discussion, see references 4 and 5. Note the absence of engine dynamics in the linearized equations of motion. This problem is rectified by matching a model to actual thrust transients.

Proper Engine Model Selection

To allow for engine spool-up/spool-down dynamics, a linear model was matched to thrust transients obtained from a high fidelity engine simulation. A second-order model provides reasonably accurate matching of dynamics,

using thrust and its derivative as state variables and throttle position as the input. The result is a model that is defined by three engine response parameters:

$$\begin{bmatrix} \dot{T} \\ \ddot{T} \end{bmatrix} = \begin{bmatrix} 0 & 1 \\ -\omega_n^2 & -2\zeta\omega_n \end{bmatrix} \begin{bmatrix} T \\ \dot{T} \end{bmatrix} + \begin{bmatrix} 0 \\ K_{Tss} \end{bmatrix} \delta_T$$

Figures 9 and 10 show validation of the second-order engine model and illustrate the match of this model with $\omega_n^2 = 2.5$, $\zeta = 0.802$, and $K_{Tss} = 250$ to thrust transients from the high fidelity simulation. The steady-state throttle lever setting of 20 percent was chosen for the transients because of its close proximity to trim throttle lever settings for several landing configurations.

Although the engine model does not have to be exact for regulator design, it should be conservative. The model parameters should err in a direction that will contribute to increased closed-loop stability. Such a conservative model is governed, for the B-720 and presumably any jet transport, by three parameters according to the following rules:

1. Select an engine natural frequency (ω_n) lower than the best guess to overestimate lag between throttle command and thrust response. An underestimated lag will act to destabilize the closed-loop system.
2. Select the best-guess damping coefficient (ζ), as it has minimal destabilizing influence if in error.
3. Select a steady-state thrust gain (K_{Tss}) larger than the best guess. Otherwise, the controller will act as though it has less actuator authority than it truly does, increasing loop gain and contributing to instability.

Several varying engine models were examined, revealing that a system conservative in each parameter provides gains by way of the LQR algorithm that provide good closed-loop response characteristics.

Note that a conservative selection of natural frequency will result in a match closer to spool-down dynamics. A more sophisticated model that matched spool-up dynamics just as well would yield a slightly more responsive controller.

Open-Loop Dynamics and Controllability

The combined linear aircraft and engine model resulted in open-loop dynamics that closely matched those of the high fidelity nonlinear simulation (appendix A). Open-loop roots are shown on the z-plane in figure 11 for the 50 Hz discrete-time version implemented on the piloted simulation. Refer to reference 6 for z-plane attributes. Characteristics of the natural modes for the linear model are summarized in table 1.

Controllability of both longitudinal and lateral-directional dynamics is assured by the B-720's satisfaction of the necessary conditions described earlier. That is, the parameters necessary to specify a given terminal flight condition (β, ϕ, V, θ) are independently attainable.

Optimal Controller

The combined aircraft and engine model of appendix A was used to iterate to an acceptable regulator by varying LQR weights and thus the cost function. For a model normalized according to the multipliers in table 2, the LQR weights of table 3 provide acceptable regulation.

It is important to realize that selection of greater weights on each of the dynamic modes will provide "tighter" control but only at the expense of decreased robustness to variations in system parameters. Also, it is futile to increase the weights on the short period and roll modes because they are difficult to excite directly by the engines.

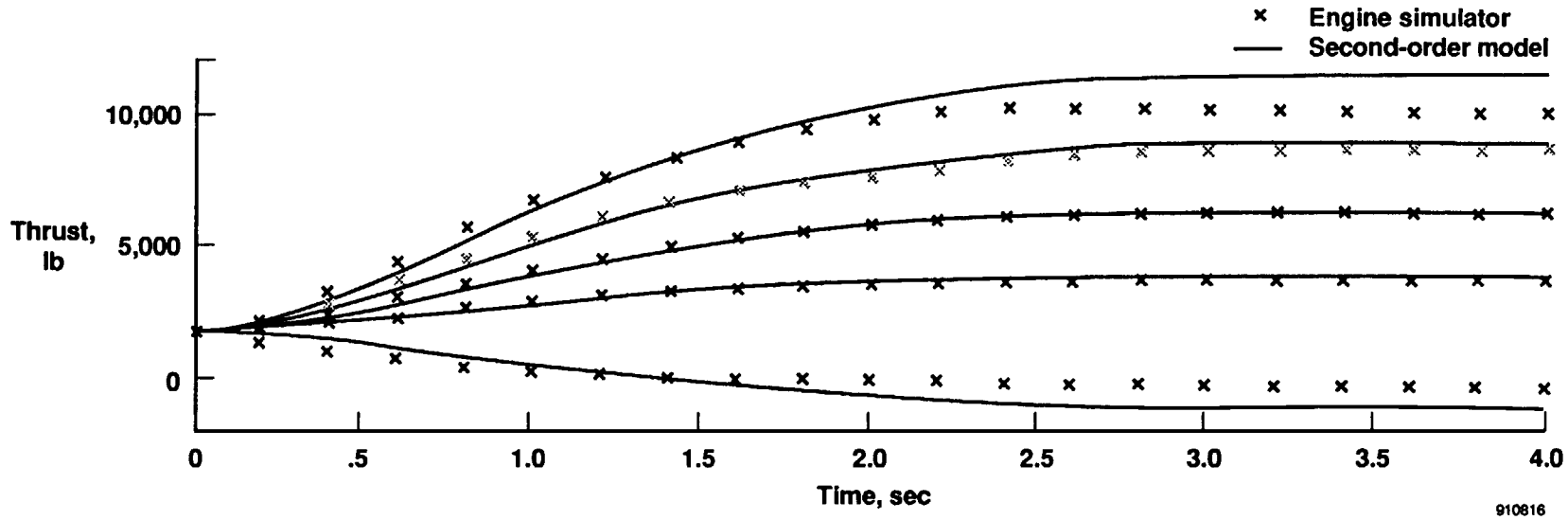

Figure 9. The B-720 engine transients from 20 percent throttle command, 4000 ft/0.28 *M*.

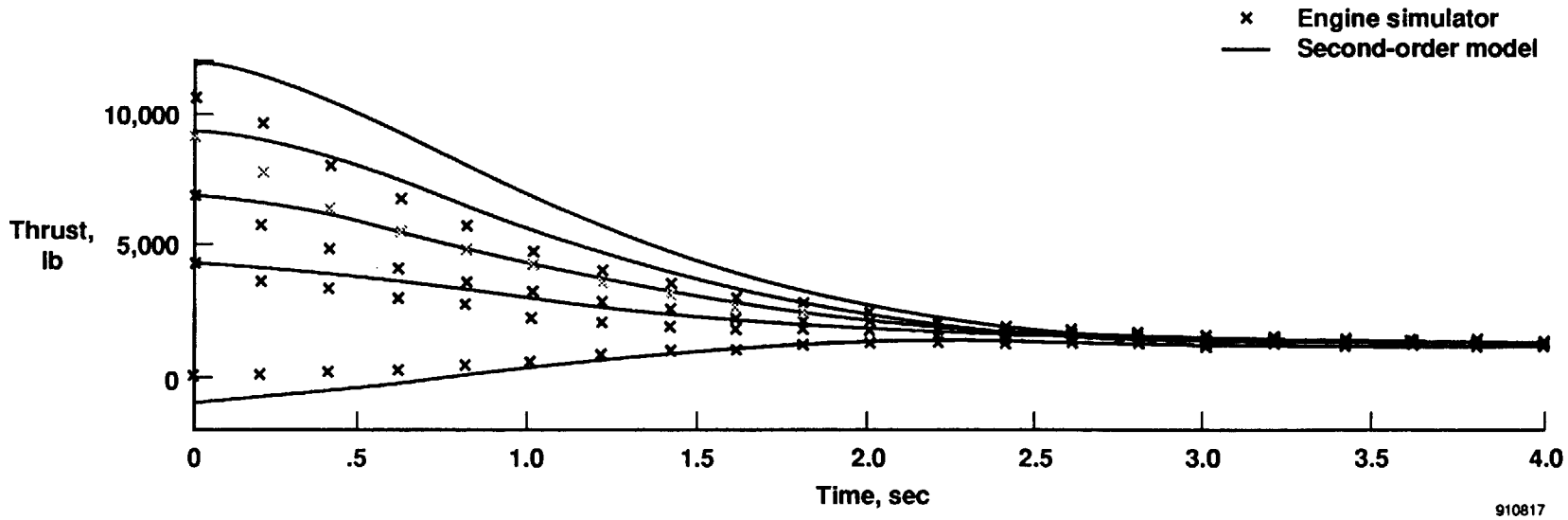

Figure 10. The B-720 engine transients to 20 percent throttle command, 4000 ft/0.28 *M*.

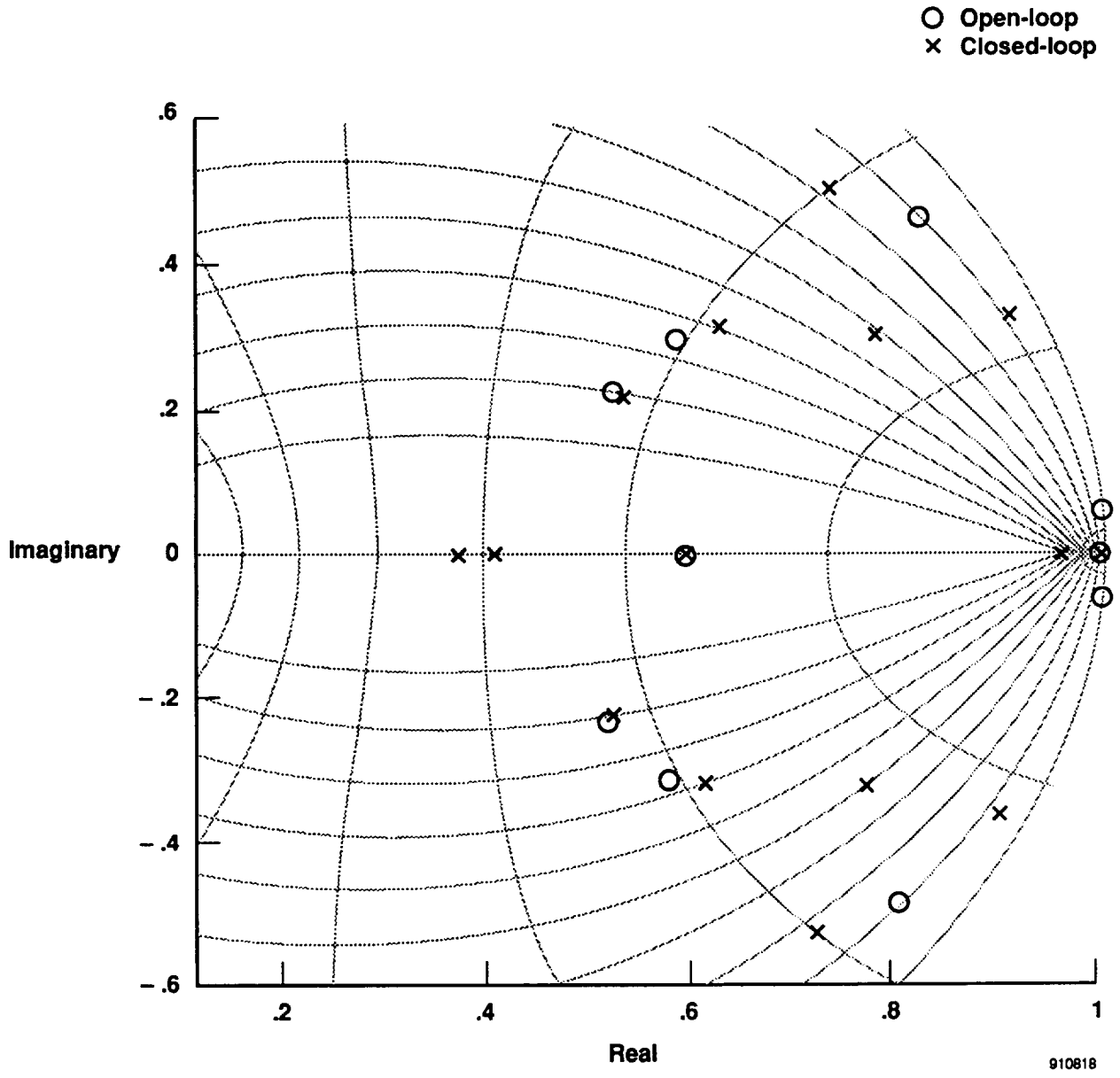

Figure 11. z-plane discrete time, open-loop, and closed-loop roots.

Table 1. Characteristics of the open-loop aircraft dynamic modes.

Mode	Period or τ sec	ζ	Stable
Short period	10	0.7	Yes
Phugoid	57	0.01	Yes
Dutch roll	6.1	0.10	Yes
Spiral	68	---	Yes
Roll	1.2	---	Yes

Table 2. Normalizing multipliers for aircraft equations of motion.

Dimension	Normalized (multiplied by)
Angle, rad	0.001
Force, lb	5906
Distance, ft	1
Throttle setting, %	0.1

Table 3. Design linear quadratic regulator weights.

Mode	Weight
Short period	1
Phugoid	10
Dutch roll	200
Spiral	0.5
Roll	1

The final gain matrix for full-state feedback is presented in appendix B. It was found that eliminating several of the feedback paths results in no degradation of closed-loop performance. In particular, it is not necessary to feedback engine parameters. This result is desirable because thrust is difficult to measure. Furthermore, altitude and heading can be eliminated unless it is desired to "hold" either quantity in the sense of an autopilot. The remaining eight quantities prove necessary and result in the following reduced feedback gain matrix:

$$K = \begin{array}{c} \begin{matrix} q & \alpha & V & \theta & p & r & \beta & \phi \end{matrix} \\ \begin{bmatrix} 594 & -467 & 2.6 & 780 & 93.9 & 584 & 91.6 & 125 \\ 1750 & -1290 & 2.1 & 2345 & 55.3 & 344 & 54.0 & 73.4 \\ 1750 & -1290 & 2.1 & 2345 & -55.3 & -344 & -54.0 & -73.4 \\ 594 & -467 & 2.6 & 780 & -93.9 & -584 & -91.6 & -125 \end{bmatrix} \end{array} \begin{matrix} \delta_{Tol} \\ \delta_{Til} \\ \delta_{Tir} \\ \delta_{Tor} \end{matrix}$$

Closed-loop roots were superimposed on the open-loop roots (figure 11). Refer to appendix C for movement of roots with longitudinal, lateral, and combined regulation.

Pilot interface parameters were selected using the linear simulation to arrive at estimated values and the nonlinear piloted simulation to fine-tune to reasonable handling qualities. The final values submitted for handling qualities evaluation are given in table 4.

Table 4. Pilot interface parameter values.

Parameter	Value
q_{stick}	0.25
pitch limit	16000/aircraft gross weight
T_s	0.02
p_{stick}	−0.25
bank limit	6,000,000/I_{zz}

Figure 12 illustrates the final version of the propulsion-only controller. Note the limiters following each regulator output and the purpose they serve in establishing a control hierarchy with lateral commands taking precedence over longitudinal. Here the rationale was that survivability in the flare will be maximized by a wings-level touchdown. Furthermore, physics dictate that reducing sink rate is best accomplished at wings-level flight. Preliminary limits were set as a function of throttle lever angle, a criteria that will likely be unacceptable for implementation on a real aircraft. Synthesis of throttle lever position with the command structure was not investigated but would certainly improve performance by providing the capability of controlling pitch and velocity independently.

Closed-Loop Performance

A good measure of performance for the closed-loop system before piloted simulation is its response to certain initial conditions, disturbances such as wind gusts, and synthetic pilot commands. After the initial design, it was discovered that the batch linear simulation indicated that much higher lateral gains would be required for adequate control than the nonlinear piloted simulator actually required. In fact, the higher lateral gains were found to exhibit unacceptable closed-loop performance on the piloted simulator, resulting in a nearly unstable system.

Reduction of the overall lateral-directional control effort using smaller dutch roll and spiral weights yielded the final gain matrix discussed in the Optimal Controller section and provided adequate lateral closed-loop performance on the piloted simulator. The piloted results are summarized in the Manned Simulation and Pilot Evaluation sections. By way of comparison and to illustrate the deviation between the two simulations, the linear closed-loop response

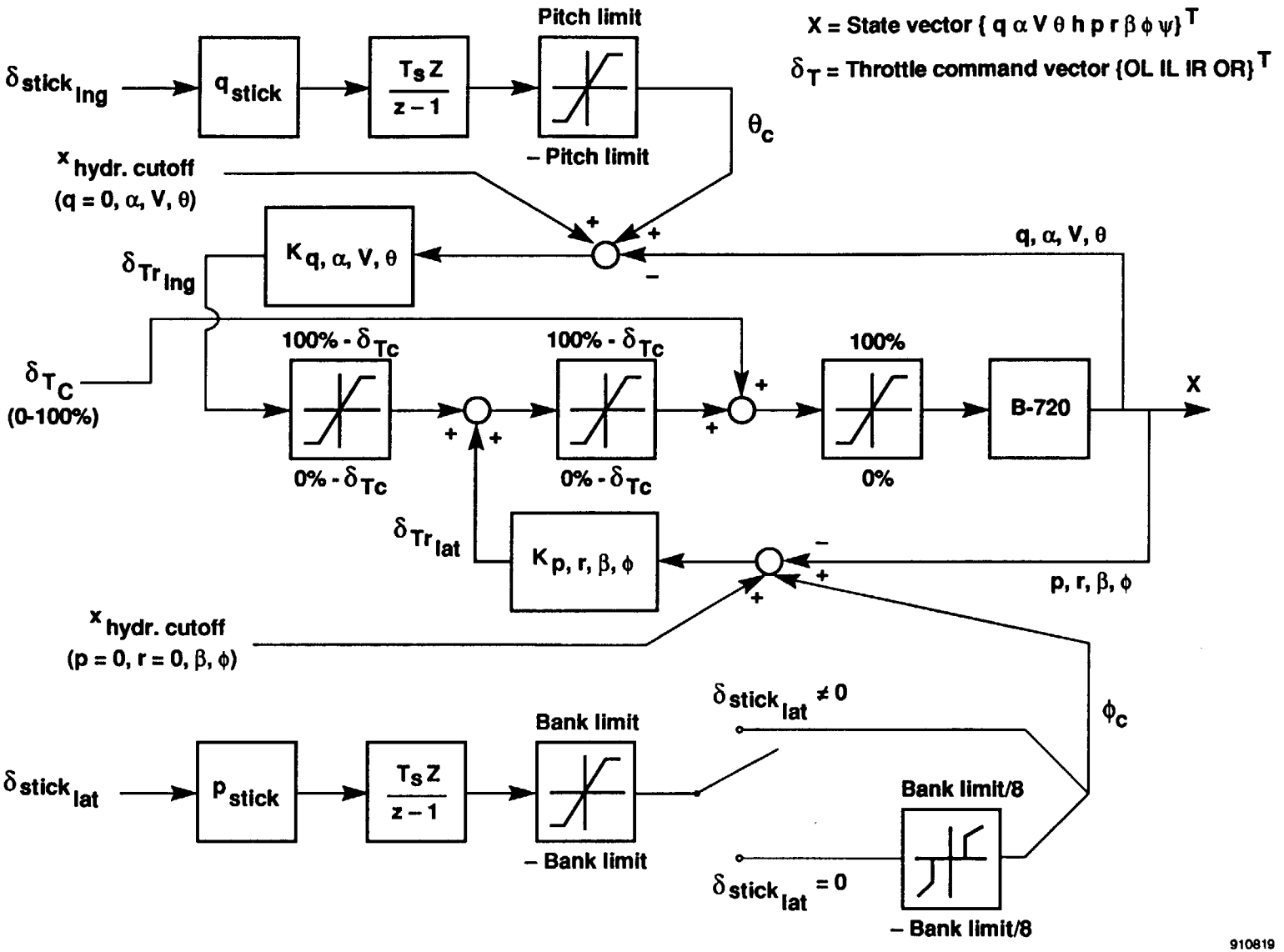

Figure 12. Block diagram of Boeing 720 linear quadratic regulator propulsion-only controller.

for the final gain design using the set of conditions listed in table 5 is presented in figures 13 to 21. These figures present the predicted lateral closed-loop performance with optimal propulsion-only control for evaluation conditions 1 through 7. Comparison of these predicted time-histories with the original design evaluation shows considerably less damping. The results of the next section will prove this prediction incorrect, illustrating the deviation between the two simulations.

Table 5. Conditions for evaluation of closed-loop performance.

Condition	Purpose
1. Initial pitch rate = 5 deg/sec	Evaluate phugoid damping/stability
2. Initial sideslip = 10°	Evaluate dutch roll damping/stability
3. Initial bank angle = 10°	Evaluate spiral damping/stability
4. Heavy turbulence	Evaluate general stability
5. Full-aft stick deflection	Analyze pitch performance/pitch angle hold
6. Full-forward stick deflection	Analyze pitch performance/pitch angle hold
7. Full-right/left stick deflection	Analyze roll performance/bank angle hold

The original longitudinal design performed as well on the nonlinear piloted simulator as predicted in linear batch mode. A possible reason is that the one-way coupling from lateral to longitudinal dynamics did not affect this part of the evaluation. It is also possible that the linear simulation, conducted at only 2 Hz, had sufficient lead to control the phugoid mode but not the dutch roll mode because of its higher natural frequencies.

MANNED SIMULATION

The final controller design given in figure 12 was implemented on the NASA Dryden high fidelity, real-time simulator shown in figure 22. The conditions listed in table 5 were recreated as best as possible in view of the nonideal nature of the simulator. Stripchart time histories are included in figures 23 to 29 for comparison with figures 13 to 21. Different models were used for gust-response analysis, so it is unlikely that any correspondence between the two simulations will be discernable for this part of the evaluation except the general ability of the controller to maintain aircraft attitude.

The predicted batch linear simulation and actual piloted nonlinear simulation performance for the evaluation criteria are summarized in table 6. In general, the longitudinal behavior of the piloted simulator closely matched the predicted performance. The only differences were a slight steady-state vertical speed for piloted condition 1 which could be eliminated with integral feedback and a phugoid oscillation for batch condition 6 when the engine commands were saturated.

A good correspondence between the batch and piloted lateral-directional, steady-state performance was also observed. As mentioned above, however, the piloted simulator exhibited considerably better dutch roll damping than predicted by the linear simulation. Possible causes for this discrepancy include the longitudinal/lateral-directional coupling in the piloted simulator; a violation of linearizing assumptions, such as small angles, in the batch simulator; an engine nonlinearity near 3000 lb thrust in the piloted simulator; or the fact that the second-order engine model can describe either spool-up or spool-down dynamics fairly well, but not both.

PILOT EVALUATIONS

The NASA research pilots evaluated the handling qualities for a variety of tasks. The tasks and corresponding pilot evaluations are presented in table 7. It was recommended that the simulator be operated without changing the

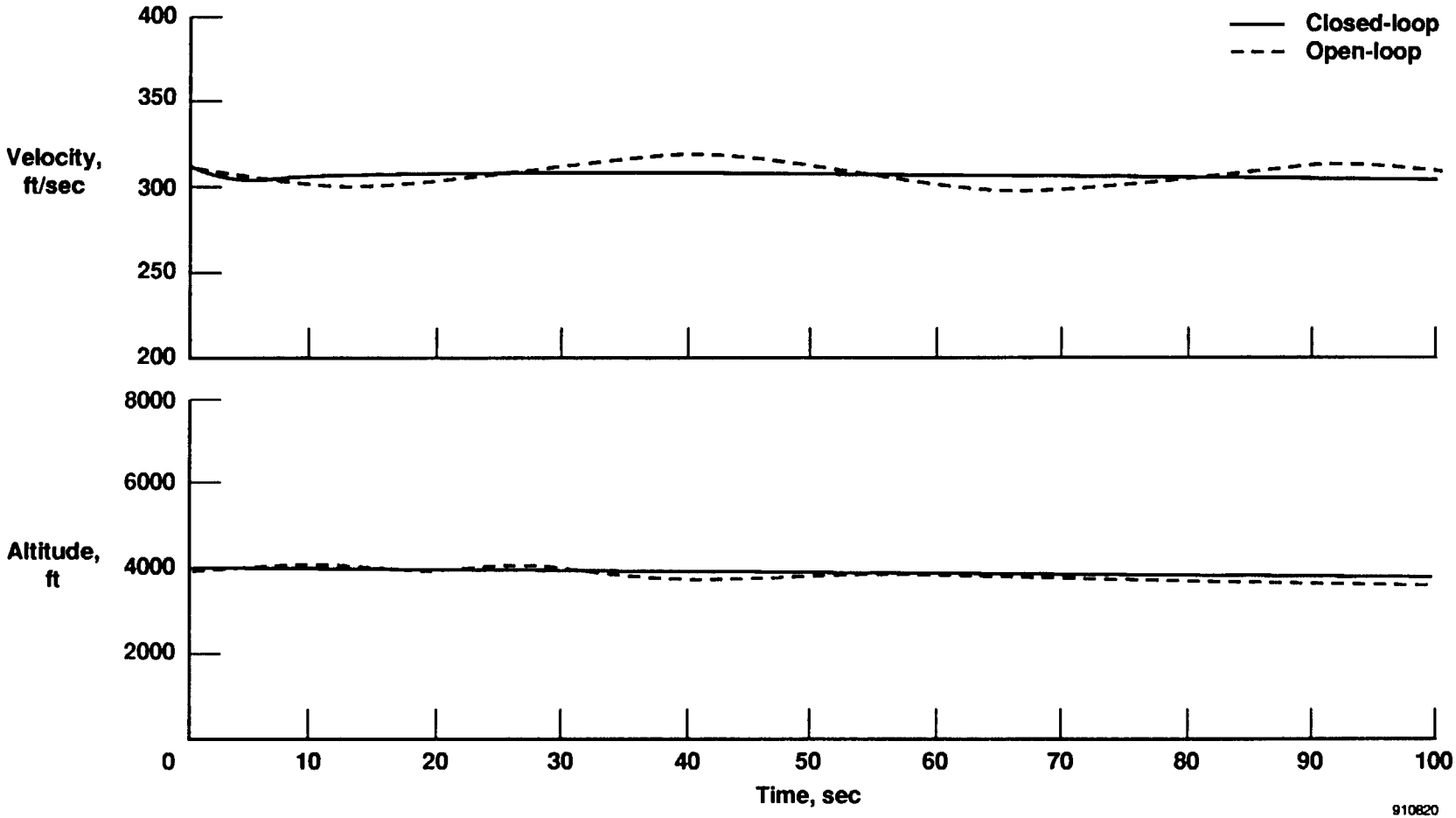

Figure 13. Evaluation condition 1: Response to an intial condition of q = 5 deg/sec.

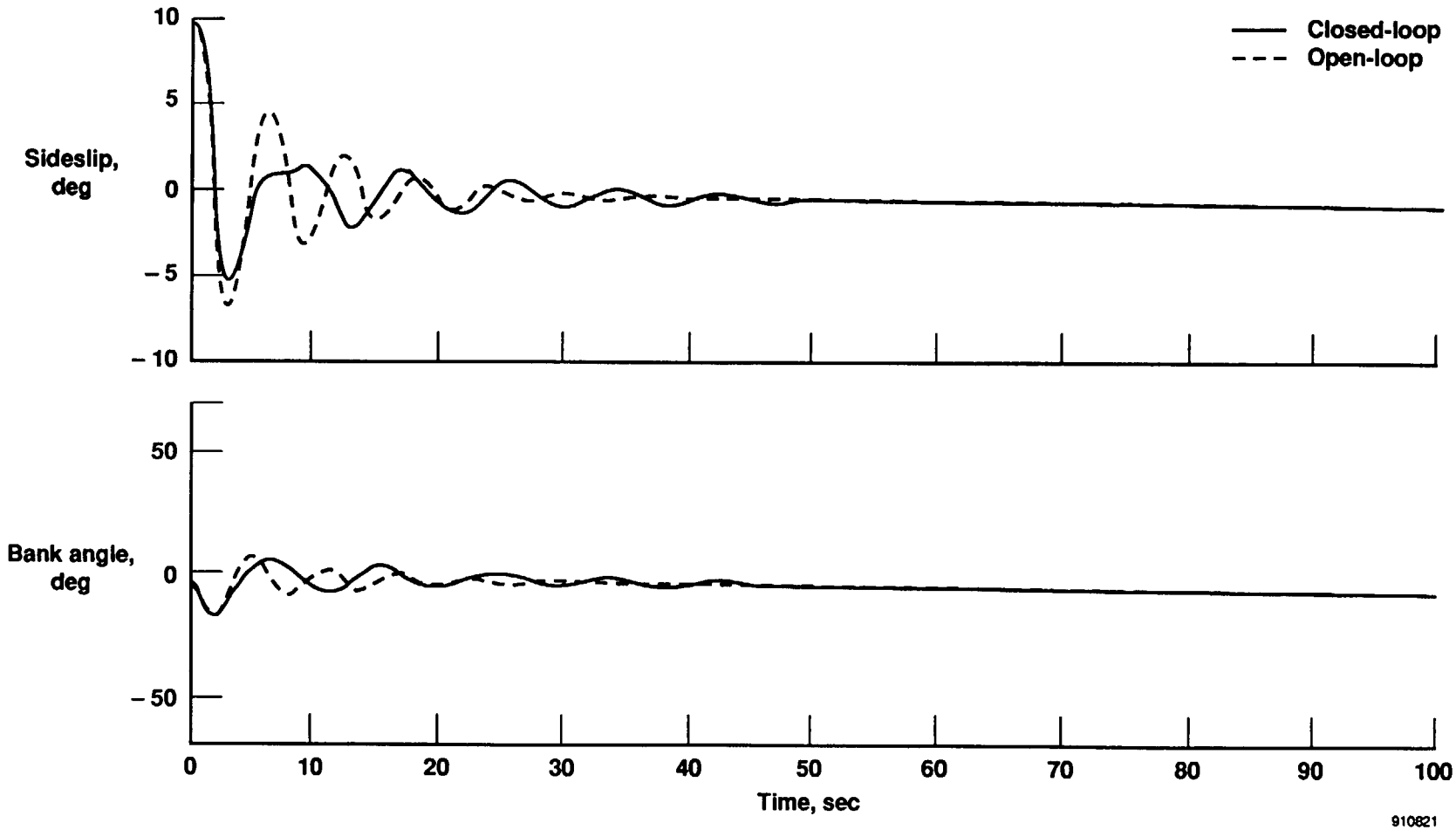

Figure 14. Evaluation condition 2: Response to an initial condition of $\beta = 10°$.

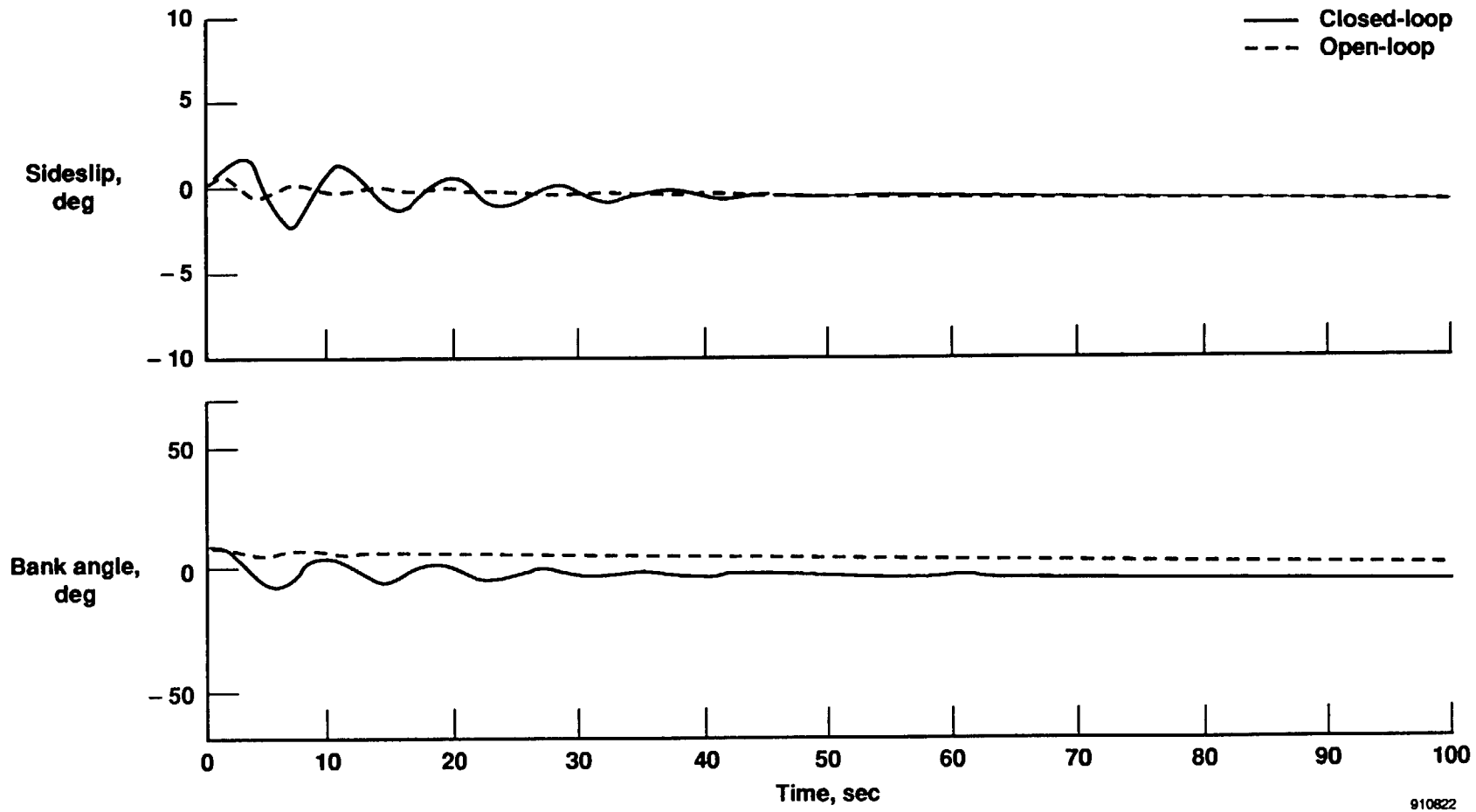

Figure 15. Evaluation condition 3: Response to an initial condition of $\phi = 10°$.

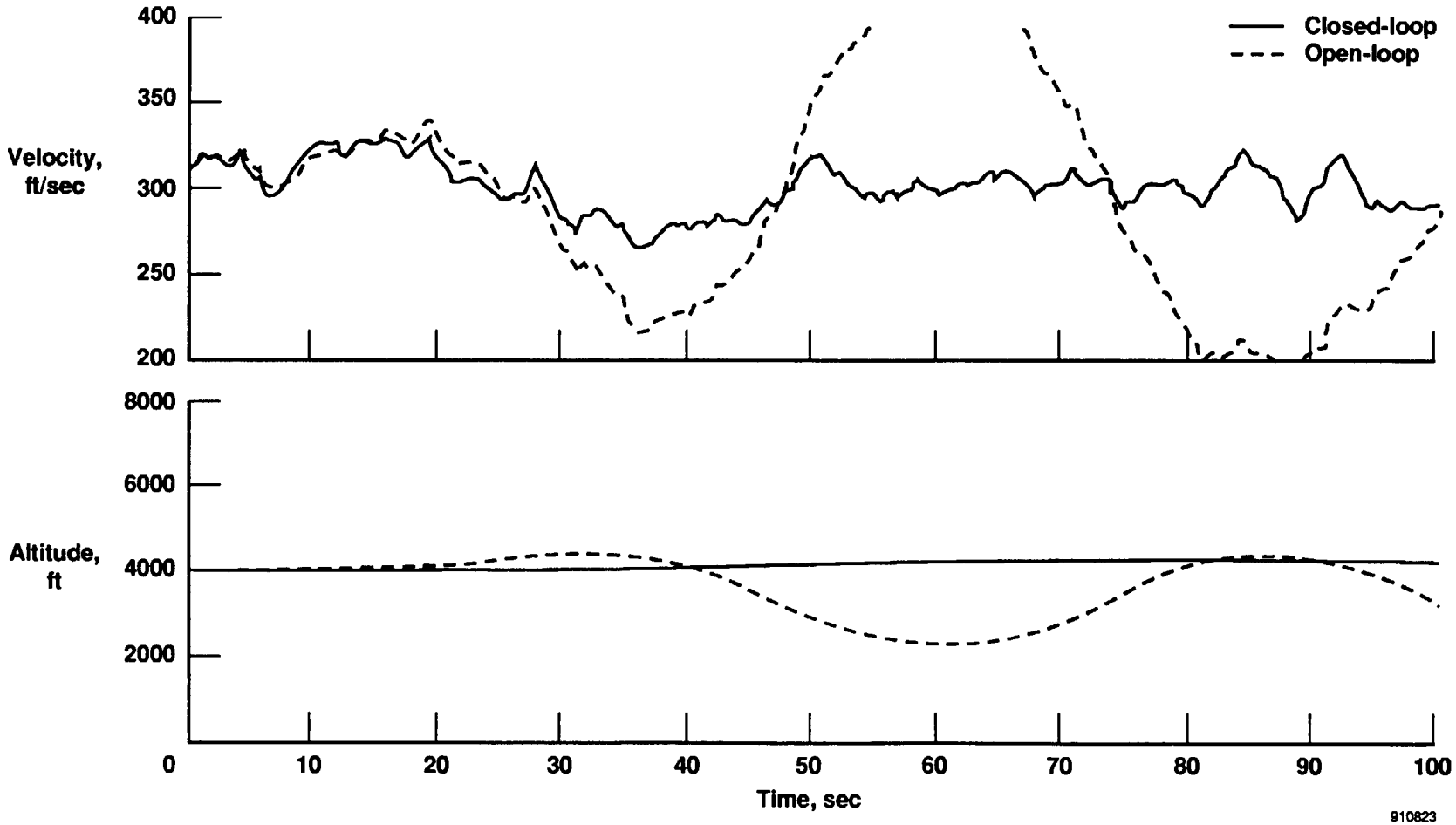

Figure 16. Evaluation condition 4a: Response to heavy turbulence, σ $\{u = 10, v = 10, w = 5\}$.

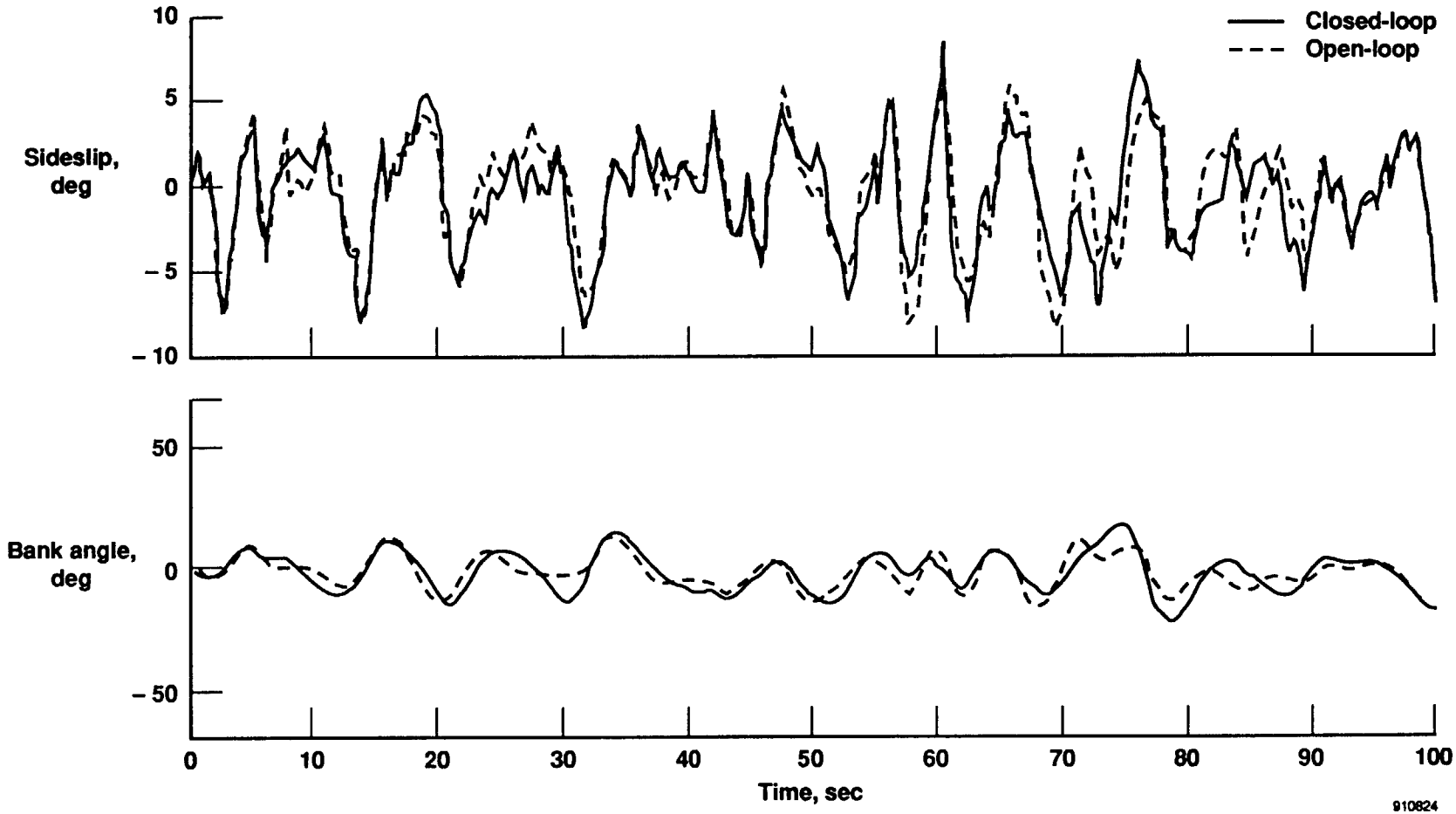

Figure 17. Evaluation condition 4b: Response to heavy turbulence, σ $\{u = 10, v = 10, w = 5\}$.

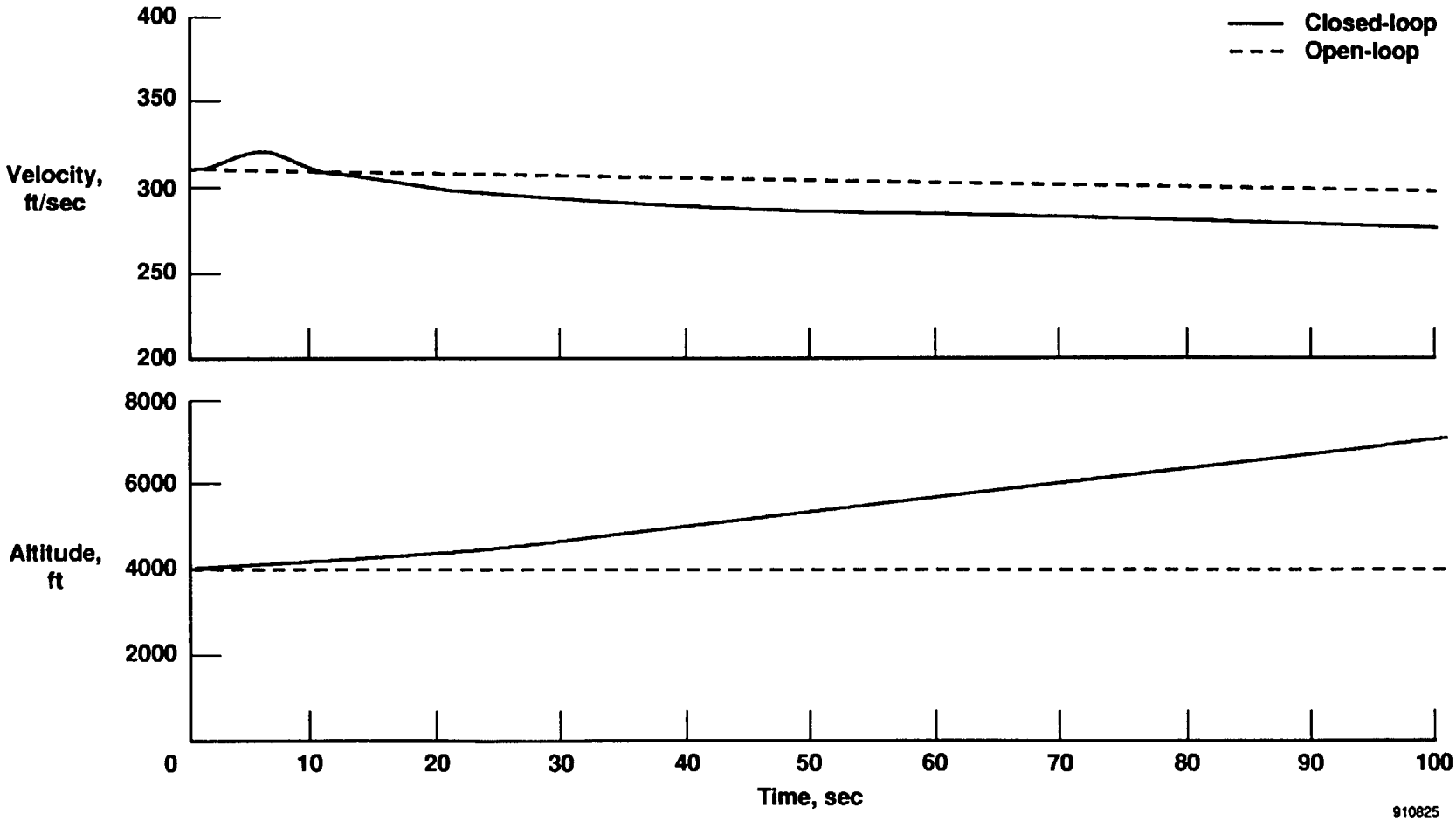

Figure 18. Evaluation condition 5: Response to full-aft stick deflection.

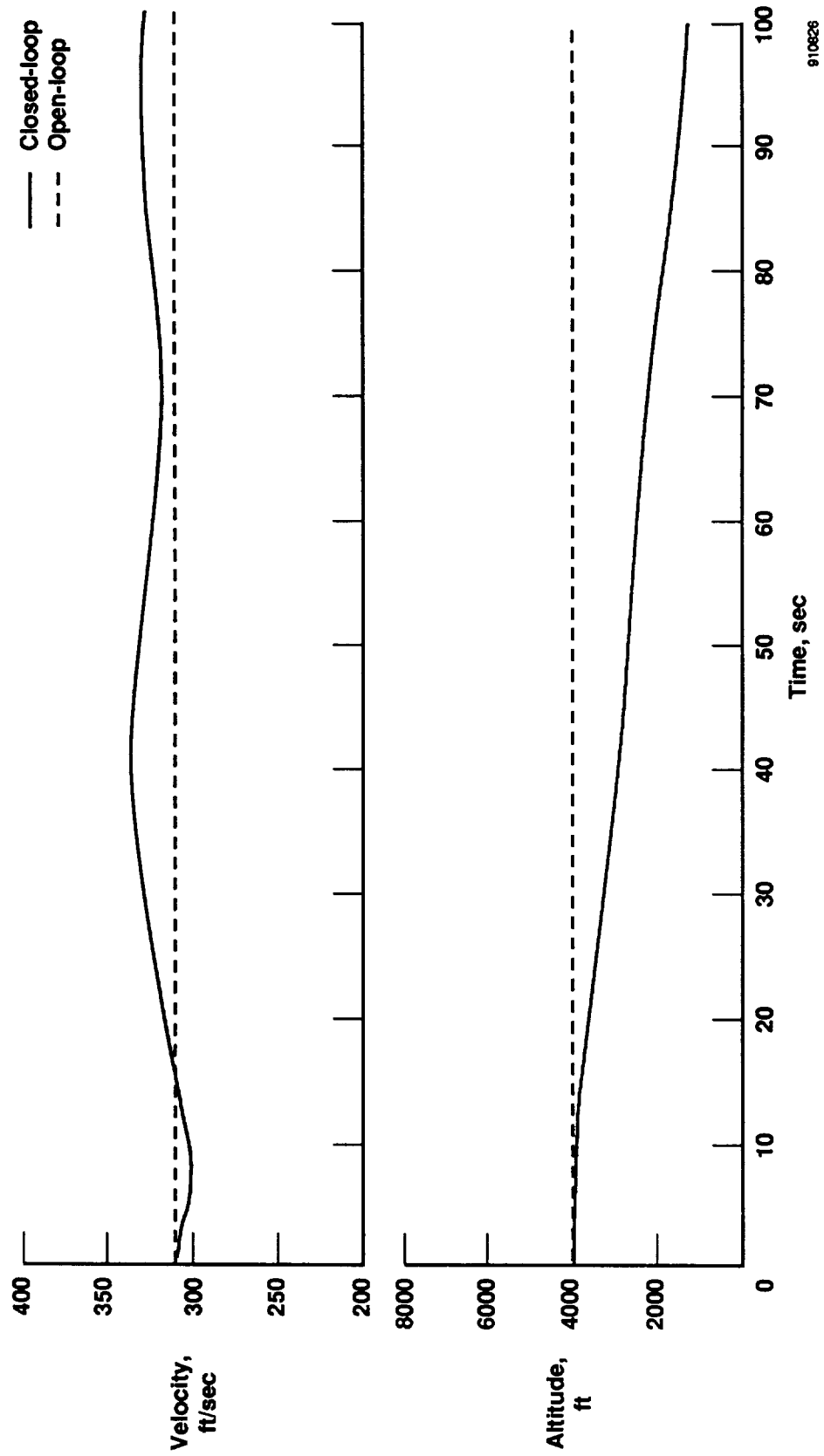

Figure 19. Evaluation condition 6: Response to full-forward stick deflection.

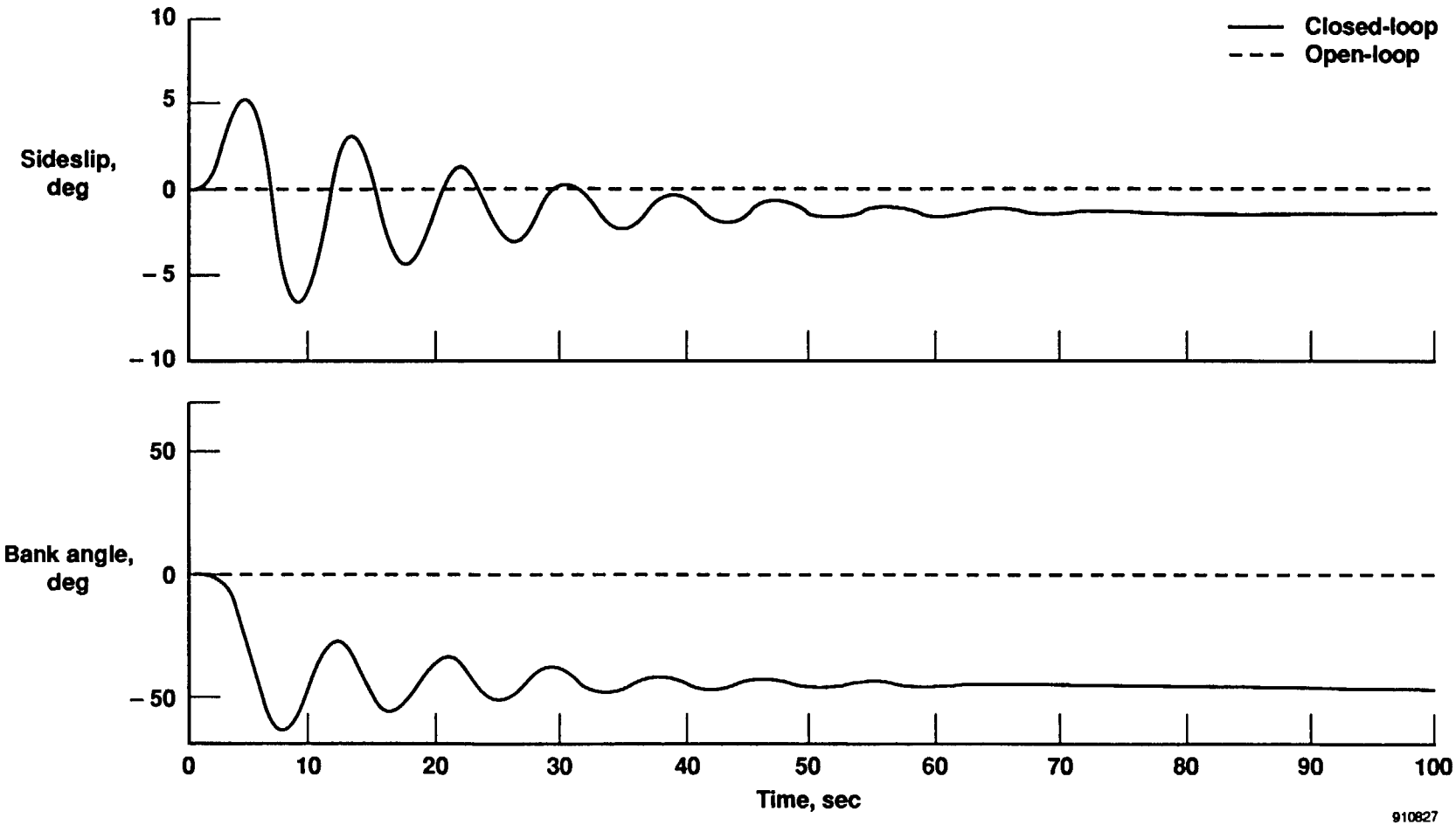

Figure 20. Evaluation condition 7a: Response to full-left stick deflection.

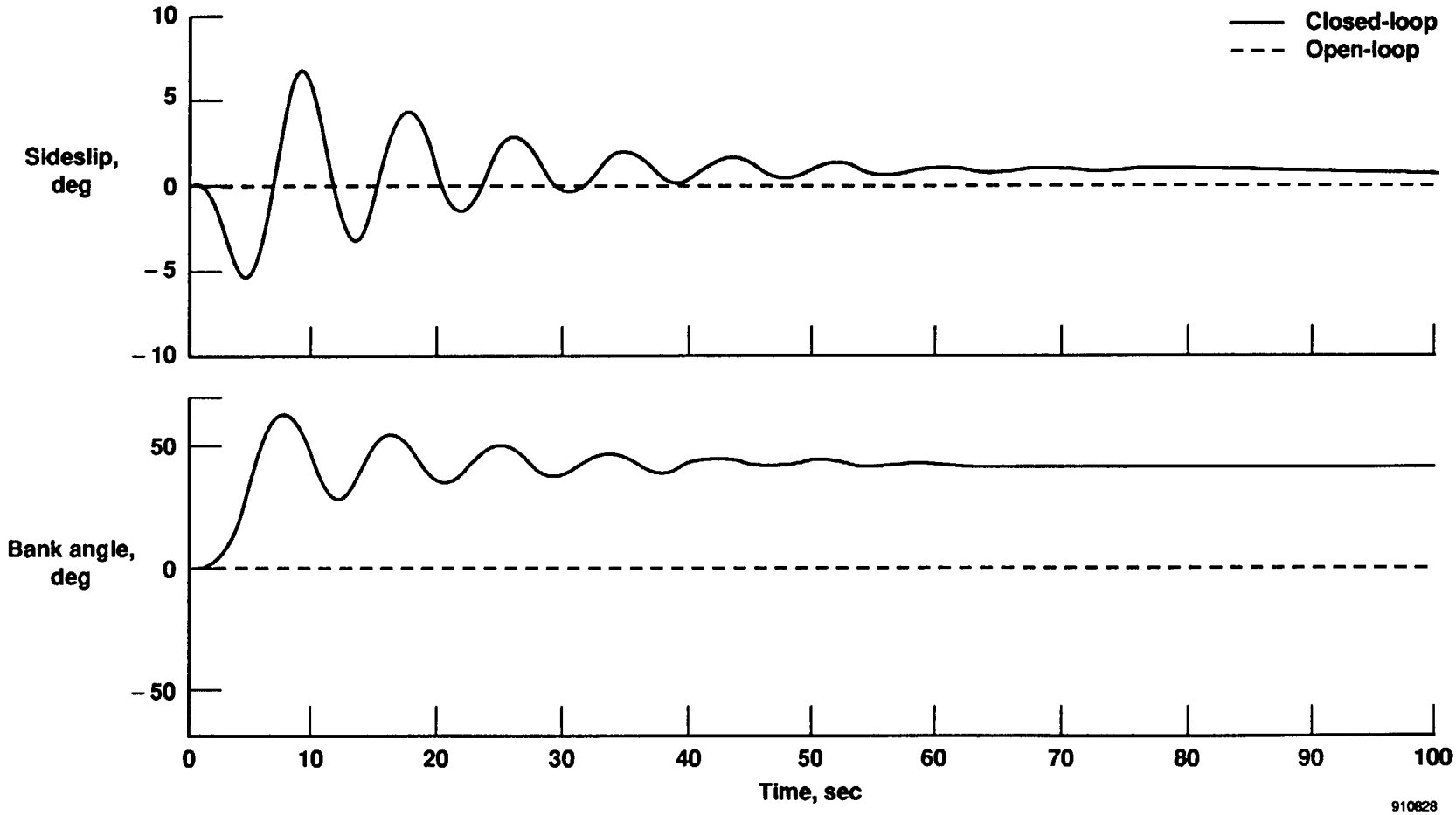

Figure 21. Evaluation condition 7b: Response to full-right stick deflection.

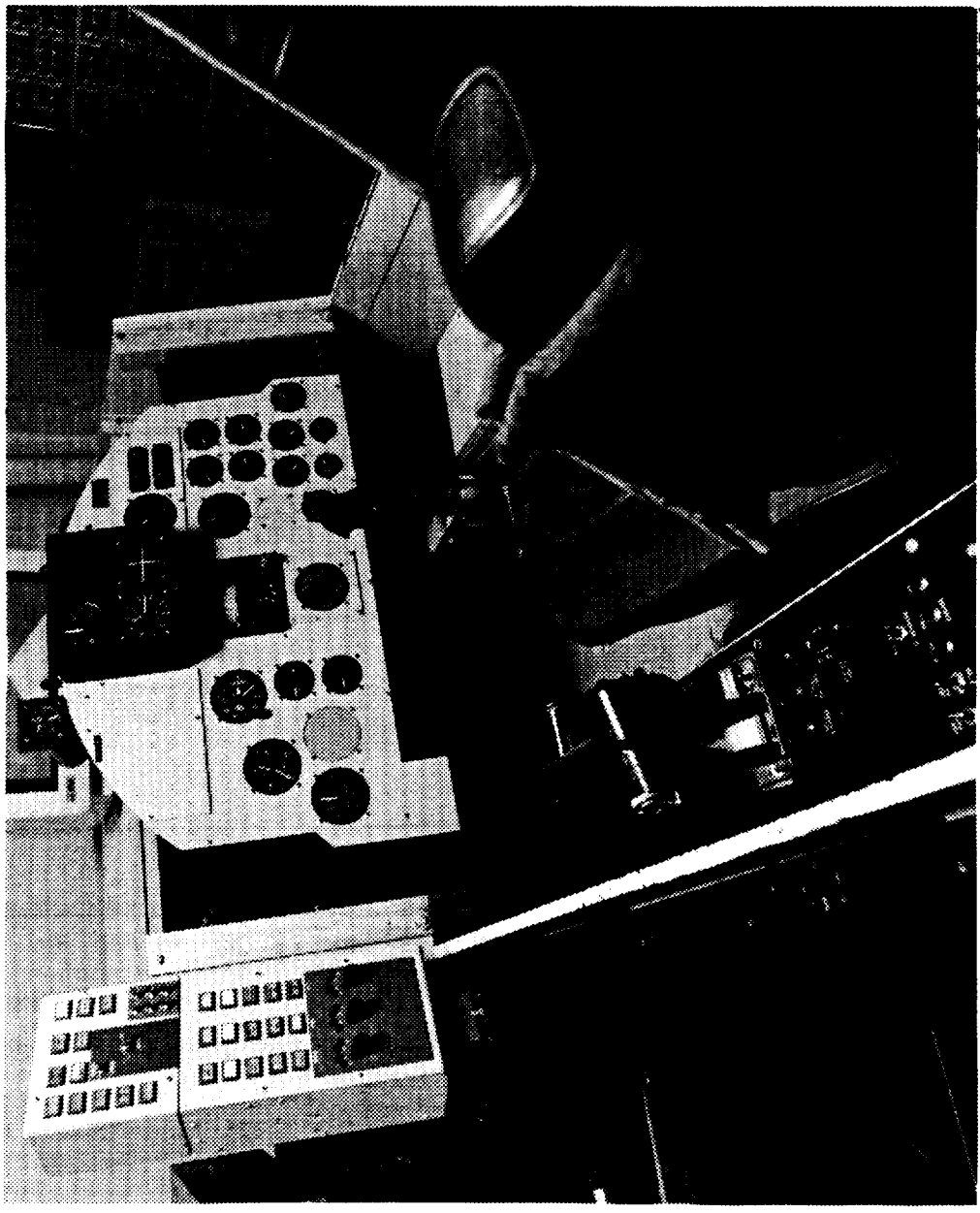

EC 90 227-1

Figure 22. Cockpit mockup of the Boeing 720 simulator.

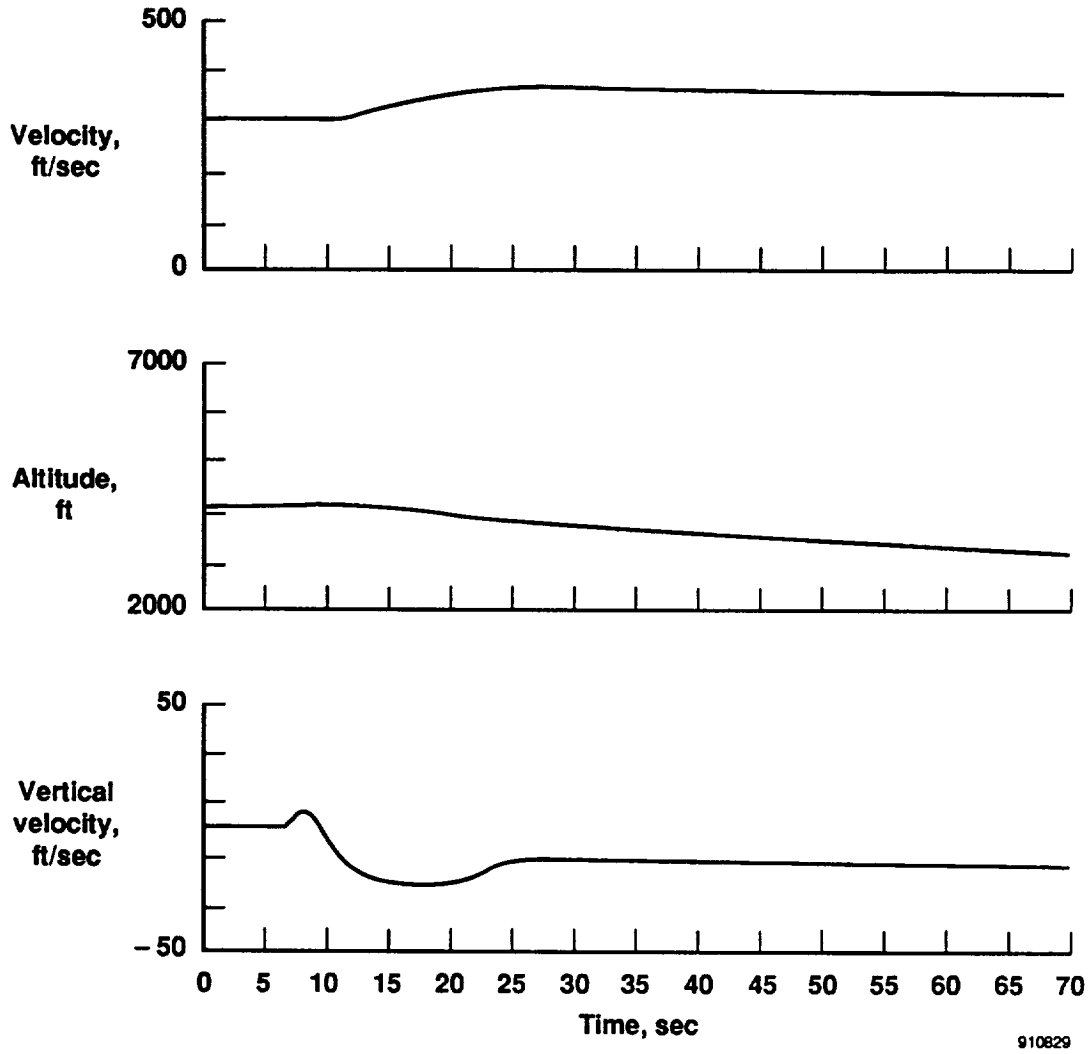

Figure 23. Closed-loop performance of the B-720 high fidelity simulator with optimal propulsion-only control for evaluation condition 1.

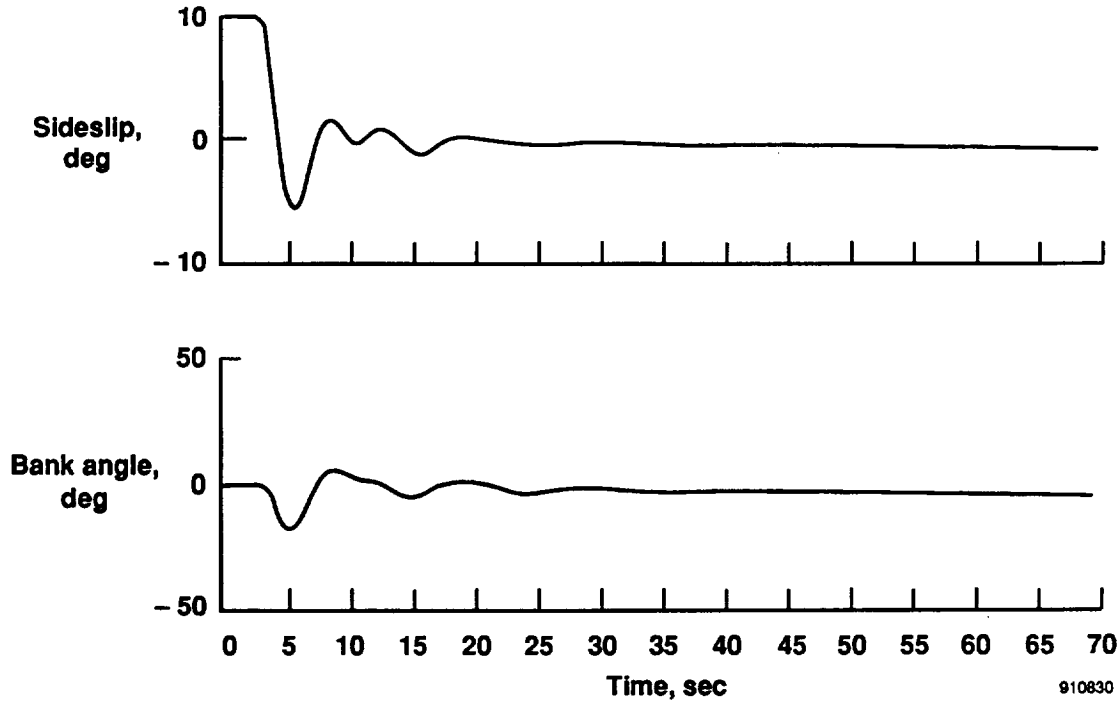

Figure 24. Closed-loop performance of the B-720 high fidelity simulator with optimal propulsion-only control for evaluation condition 2.

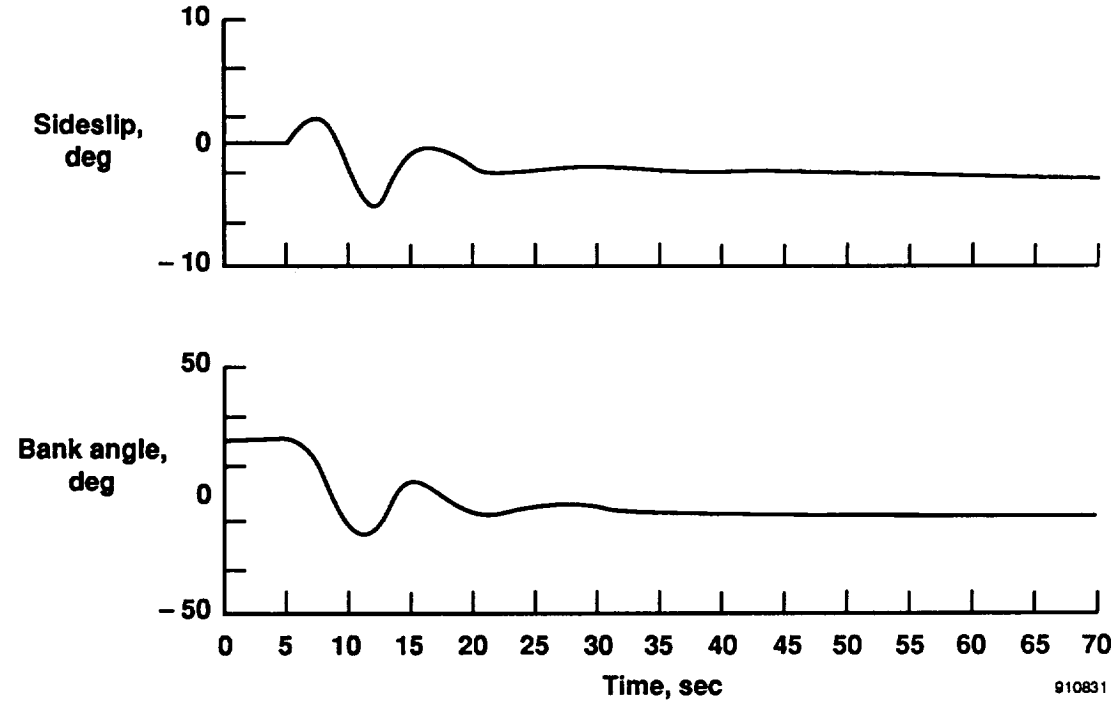

Figure 25. Closed-loop performance of the B-720 high fidelity simulator with optimal propulsion-only control for evaluation condition 3.

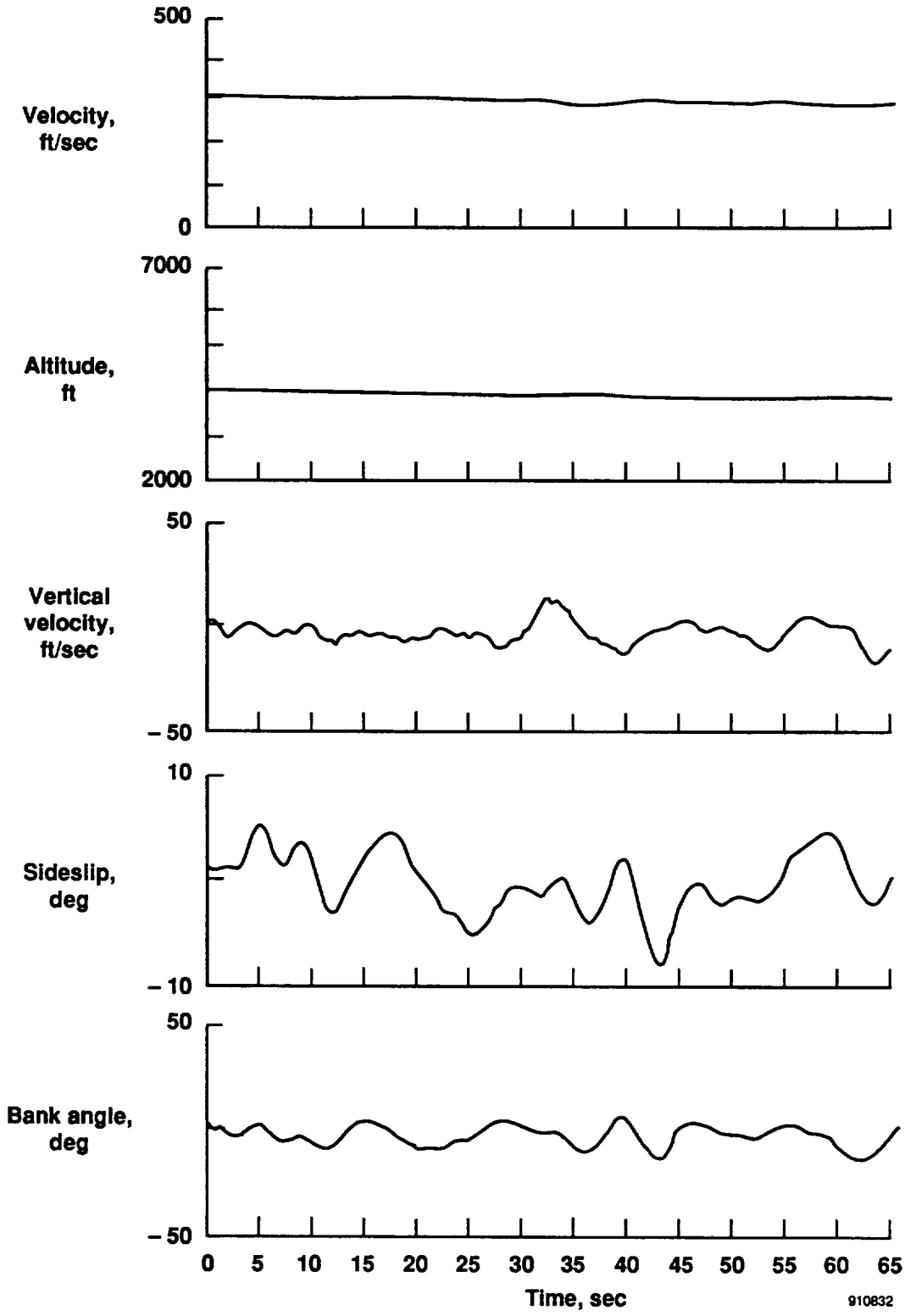

Figure 26. Closed-loop performance of the B-720 high fidelity simulator with optimal propulsion-only control for evaluation condition 4.

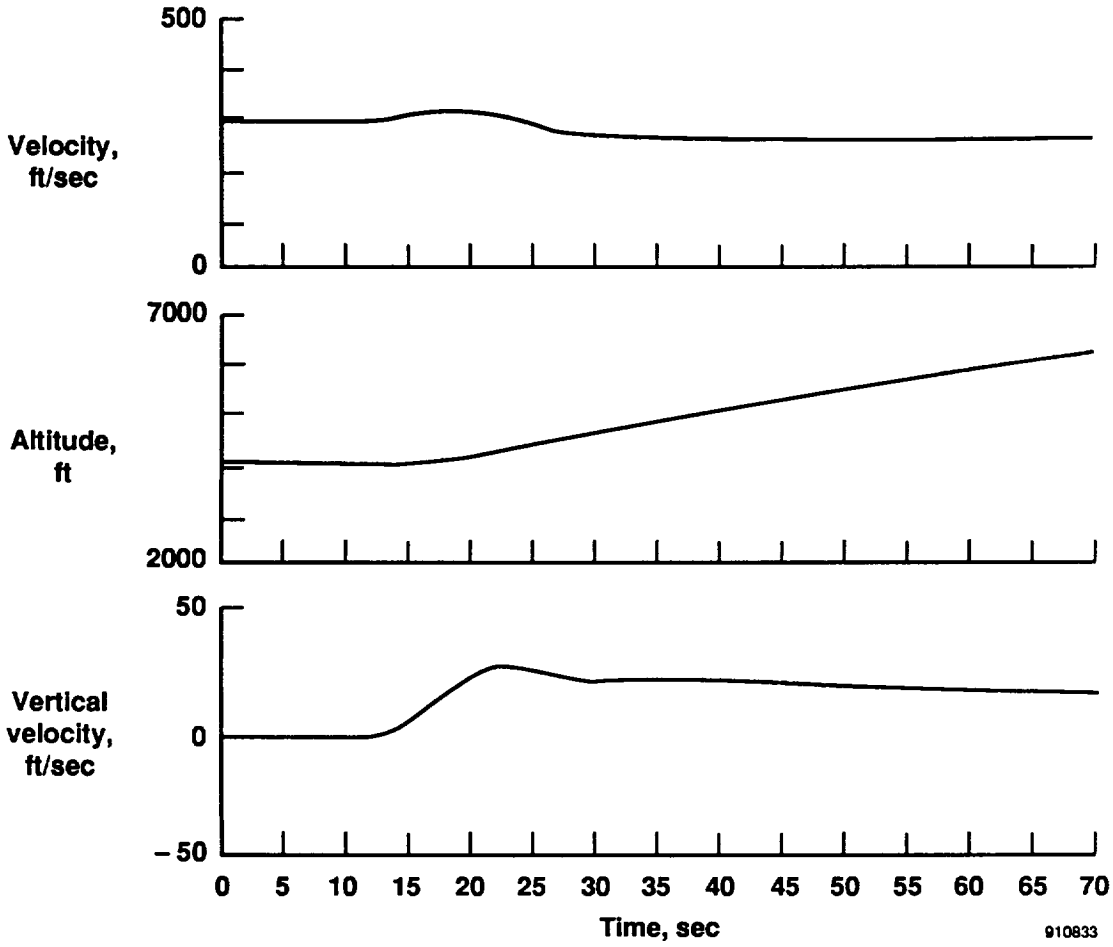

Figure 27. Closed-loop performance of the B-720 high fidelity simulator with optimal propulsion-only control for evaluation condition 5.

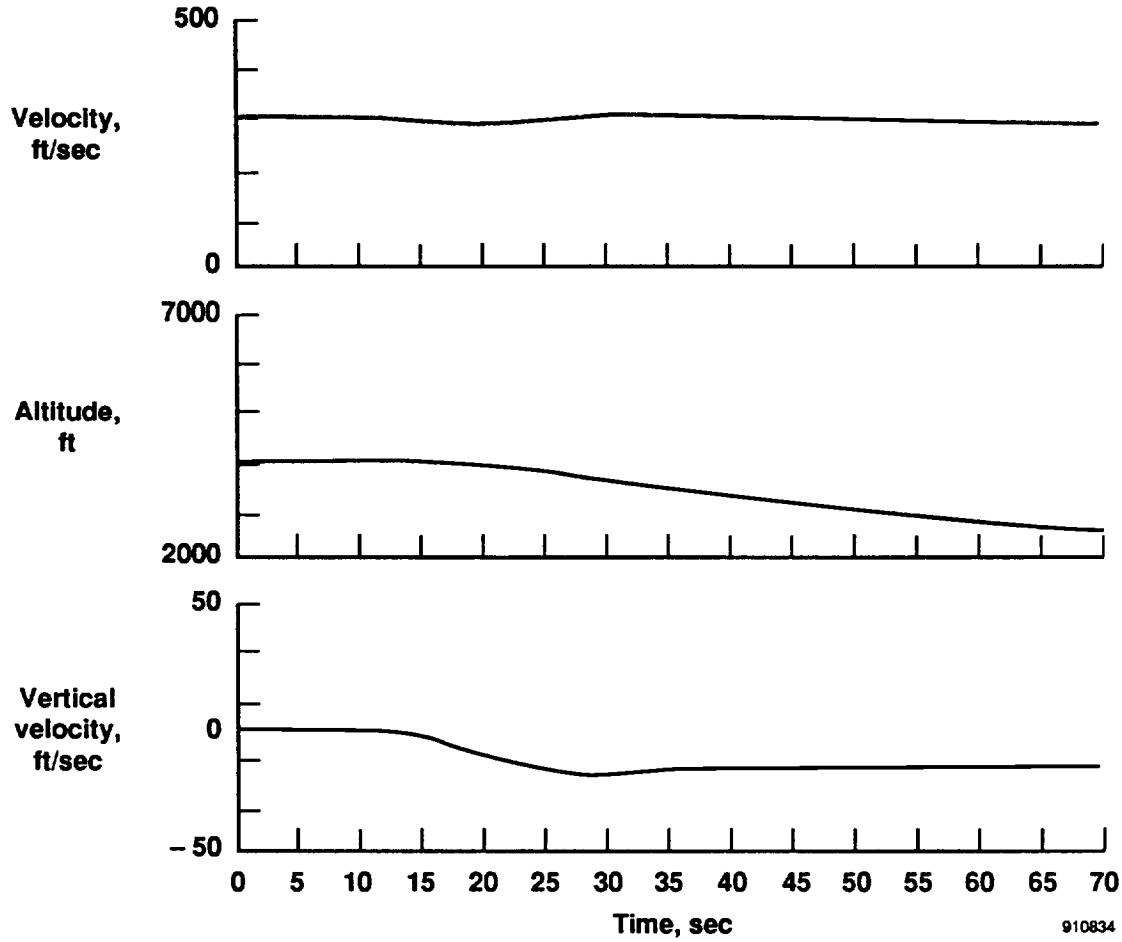

Figure 28. Closed-loop performance of the B-720 high fidelity simulator with optimal propulsion-only control for evaluation condition 6.

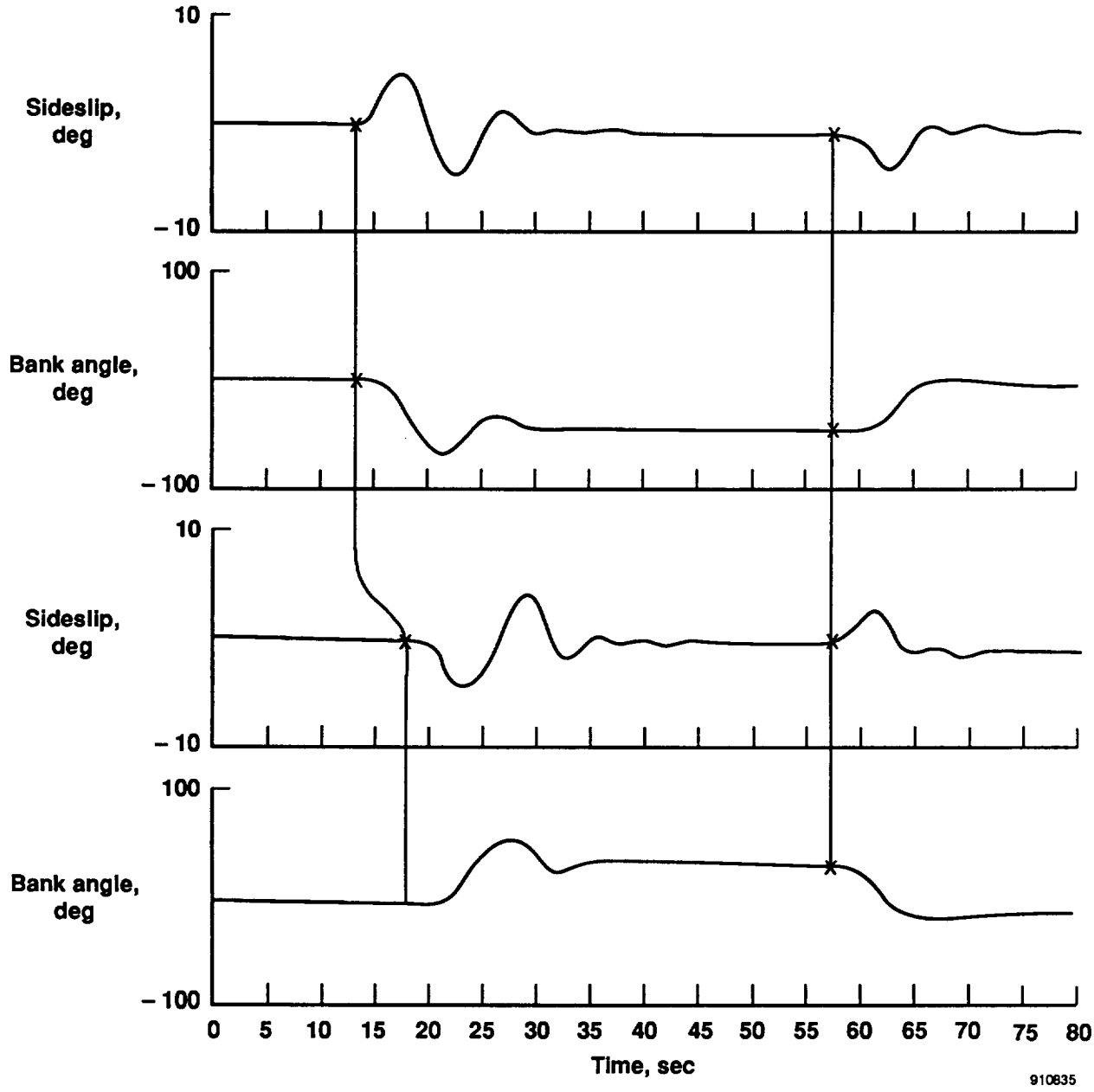

Figure 29. Closed-loop performance of the B-720 high fidelity simulator with optimal propulsion-only control for evaluation condition 7.

Table 6. Closed-loop performance for evaluation criteria.

Condition	Steady-state performance			
	Batch linear simulation		Piloted nonlinear simulation	
1. Initial pitch rate = 5 deg/sec	V = 312 fps	h = 4100 ft	V = 380 fps	h = variable
2. Initial sideslip = 10°	β = 0°	ϕ = 0°	β = 0°	ϕ = 0°
3. Initial bank angle = 10°	β = 0°	ϕ = 0°	β = −1.8°	ϕ = −5°
4. Heavy turbulence	V = ±30 fps	h = variable	V = ±20 fps	h = variable
	β = ±8°	ϕ = ±20°	β = ±8°	ϕ = ±15°
5. Full-aft stick	V = 292 fps	h = 2400 fpm	V = 290 fps	h = 2400 fpm
6. Full-forward stick	V = variable	h = 1400 fpm	V = 330 fps	h = 1300 fpm
7. Full-right/left stick	β = 1/−1°	ϕ = 43/−43°	β = 0°	ϕ = 41/−41°

Table 7. Pilot evaluations.

Task	Flight condition	Pilot comments
Altitude change	Up-and-away	Achieves and holds a rate of climb, but return to level flight is difficult.
Velocity change	Up-and-away	Somewhat "mysterious."
Heading change	Up-and-away	Holds steady-state turns well, but it is difficult to maintain altitude. Roll rate command is more intuitive than the bank angle command.
Establish sink rate	Approach and landing	Acceptable, upon conquering the learning curve. Flightpath angle command is preferable, but it is unsure how the angle will be measured reliably.
Hold ground track	Approach and landing	Acceptable, but lightly damped roll is a bit bothersome.
Flare	Approach and landing	Too much lag. It will require some practice to determine when to initiate flare.

nominal throttle setting because of the lack of translation of throttle lever position into a velocity command. For more detailed discussion, refer to Recommendations for Further Work. Furthermore, adjustments in the throttle lever positions alter the limiter bounds and will potentially degrade performance. At the very least, throttle commands will be washed out by the longitudinal regulator as it is currently implemented.

In general, the handling qualities evaluation of this prototype optimal controller was favorable. As anticipated, the 2- to 4-second control lag because of engine response presented a problem. Better control was maintained in the landing task, where stick inputs were smaller and typically impulsive thereby reducing PIO tendencies.

Up-and-away gross maneuvers required fairly low pilot workload to maintain lateral-directional control. The wings-leveling tendency below a specified bank angle blended well with the pseudoroll-rate command/bank angle hold feature. Longitudinal control presented more of a problem, however, as the pseudopitch-rate command made it difficult to find level flight. It became even more apparent that revisions were needed in this area when the simulator achieved bank angles sufficient to induce coupling to longitudinal dynamics. The pilots would instinctively apply aft stick to counter sink rate and upon rolling out found it difficult to reestablish level flight. A solution might use a blended implementation similar to the lateral-directional command interface.

RECOMMENDATIONS FOR FURTHER WORK

Although significant progress was made in the implementation of an optimal propulsion-only controller for the B-720 aircraft, considerable room remains for further research. The following recommendations constitute several areas neglected during this abbreviated study:

1. Investigate methods for permitting deviations in throttle position from equilibrium to translate into velocity commands in the regulator loop, so the pilot may control velocity independent of pitch. This change will provide a more conventionally handling aircraft during the landing task, where glide slope is typically controlled with the throttles.

2. Develop a time-optimal pilot interface to provide a pilot control bandwidth limited only by engine response. In other words, a better solution to the inversion of the DC-gain matrices should be investigated.

3. Evaluate the capability of particular aircraft to recover from control surface biases locked in at the time of hydraulic failure. Maximum deflections, asymmetries, or both, for which the aircraft is trimable with engines alone should be identified.

4. Examine other common flight tasks, for example, landing in a strong but steady crosswind.

5. Act on suggestions by NASA pilots for improved handling qualities, particularly elimination of the wandering bank angle (a coupled spiral-engine mode), and improved robustness to configuration and flight condition changes such as flaps down. Both problems should be rectified with selection of a better cost function with different LQR weights. Also, reduce pitch sensitivity and the resulting PIO tendency, possibly by going to a flightpath angle command system.

6. Bring in the United 232 pilots, and get their evaluation of the closed-loop POFCS handling qualities.

7. Implement an optimal multivariable controller on a real aircraft such as the NASA 905 (the 747).

CONCLUDING REMARKS

A propulsion-only control system was developed for the Boeing 707-720 using optimal linear quadratic regulator design techniques. Transformation of the equations of motion to modal coordinates provided a more intuitive cost

function definition. A prototype pilot interface was developed to provide sufficient authority in pitch and roll without saturating the engine commands. The entire preliminary controller was implemented on NASA Dryden's high fidelity Boeing 720 simulator, and NASA pilot evaluations were obtained. The evaluation results were favorable and included recommendations for improvement.

As previously demonstrated by Dryden engineers, the concept of propulsion-only flightpath control is quite feasible and should be seriously considered as a back-up flight control mode in future generation transport aircraft. Propulsion-only control modes can dramatically improve pilots' ability to control flightpath for the approach and landing flight condition.

While this investigation was not as comprehensive as desired because of time constraints, it did reveal several interesting problems, potential solutions, and topics for further research.

Dryden Flight Research Facility
National Aeronautics and Space Administration
Edwards, California, May 1, 1991

REFERENCES

1. Bryson, Arthur E., Jr., and Ho, Yu Chi, *Applied Optimal Control: Optimization, Estimation, and Control*, Hemisphere Publishing Corp., Washington, 1975.

2. Kailath, Thomas, *Linear Systems*, Prentice-Hall, Inc., Englewood Cliffs, 1980.

3. Franklin, Gene F., J. David Powell, and Abbas Emami-Naeini, *Feedback Control of Dynamic Systems*, Addison-Wesley, Reading, 1986.

4. McRuer, Duane, Irving Ashkenas, and Dunstan Graham, *Aircraft Dynamics and Automatic Control*, Princeton University Press, Princeton, 1973.

5. Roskam, Jan, *Airplane Flight Dynamics and Automatic Flight Controls*, Roskam Aviation and Engineering Corp., Ottawa, KS, 1979.

6. Franklin, Gene F., and J. David Powell, *Digital Control of Dynamic Systems*, Addison-Wesley, Reading, 1980.

APPENDIX A
COMBINED AIRCRAFT AND ENGINE MODEL

The combined aircraft and engine model includes both longitudinal and lateral-directional degrees of freedom. The flight condition is for a 160,000 lb gross weight, 4,000-ft altitude, and 175 kcas velocity.

Columns 1 through 9

$$A = \begin{bmatrix}
-0.8890 & -0.9790 & 0.0001 & 0 & 0 & 0 & 0 & 0 & 0 \\
1.0000 & -0.7900 & -0.0007 & 0 & 0 & 0 & 0 & 0 & 0 \\
0 & 12.9000 & -0.0121 & -32.2000 & 0.0001 & 0 & 0 & 0 & 0 \\
1.0000 & 0 & 0 & 0 & 0 & 0 & 0 & 0 & 0 \\
0 & -312.0000 & 0 & 312.0000 & 0 & 0 & 0 & 0 & 0 \\
0 & 0 & 0 & 0 & 0 & -0.9860 & 0.5490 & -2.9700 & 0 \\
0 & 0 & 0 & 0 & 0 & -0.0530 & -0.2070 & 0.7600 & 0.0021 \\
0 & 0 & 0 & 0 & 0 & 0.1050 & -0.9820 & -0.1110 & 0.1020 \\
0 & 0 & 0 & 0 & 0 & 1.0000 & 0.1120 & 0 & 0 \\
0 & 0 & 0 & 0 & 0 & 0 & 1.0100 & 0 & 0 \\
0 & 0 & 0 & 0 & 0 & 0 & 0 & 0 & 0 \\
0 & 0 & 0 & 0 & 0 & 0 & 0 & 0 & 0 \\
0 & 0 & 0 & 0 & 0 & 0 & 0 & 0 & 0 \\
0 & 0 & 0 & 0 & 0 & 0 & 0 & 0 & 0 \\
0 & 0 & 0 & 0 & 0 & 0 & 0 & 0 & 0 \\
0 & 0 & 0 & 0 & 0 & 0 & 0 & 0 & 0 \\
0 & 0 & 0 & 0 & 0 & 0 & 0 & 0 & 0
\end{bmatrix}$$

Columns 10 through 18

$$\begin{bmatrix}
0 & 0.0000 & 0 & 0.0000 & 0 & 0.0000 & 0 & 0.0000 & 0 \\
0 & -0.0000 & 0 & -0.0000 & 0 & -0.0000 & 0 & -0.0000 & 0 \\
0 & 0.0002 & 0 & 0.0002 & 0 & 0.0002 & 0 & 0.0002 & 0 \\
0 & 0 & 0 & 0 & 0 & 0 & 0 & 0 & 0 \\
0 & 0 & 0 & 0 & 0 & 0 & 0 & 0 & 0 \\
0 & 0.0000 & 0 & 0.0000 & 0 & -0.0000 & 0 & -0.0000 & 0 \\
0 & 0.0000 & 0 & 0.0000 & 0 & -0.0000 & 0 & -0.0000 & 0 \\
0 & 0 & 0 & 0 & 0 & 0 & 0 & 0 & 0 \\
0 & 0 & 0 & 0 & 0 & 0 & 0 & 0 & 0 \\
0 & 0 & 0 & 0 & 0 & 0 & 0 & 0 & 0 \\
0 & 0 & 1.0000 & 0 & 0 & 0 & 0 & 0 & 0 \\
0 & -3.5000 & -3.0000 & 0 & 0 & 0 & 0 & 0 & 0 \\
0 & 0 & 0 & 0 & 1.0000 & 0 & 0 & 0 & 0 \\
0 & 0 & 0 & -3.5000 & -3.0000 & 0 & 0 & 0 & 0 \\
0 & 0 & 0 & 0 & 0 & 0 & 1.0000 & 0 & 0 \\
0 & 0 & 0 & 0 & 0 & -3.5000 & -3.0000 & 0 & 0 \\
0 & 0 & 0 & 0 & 0 & 0 & 0 & 0 & 1.0000 \\
0 & 0 & 0 & 0 & 0 & 0 & 0 & -3.5000 & -3.0000
\end{bmatrix}$$

$$
B = \begin{bmatrix}
0 & 0 & 0 & 0 \\
0 & 0 & 0 & 0 \\
0 & 0 & 0 & 0 \\
0 & 0 & 0 & 0 \\
0 & 0 & 0 & 0 \\
0 & 0 & 0 & 0 \\
300 & 0 & 0 & 0 \\
0 & 0 & 0 & 0 \\
0 & 300 & 0 & 0 \\
0 & 0 & 0 & 0 \\
0 & 0 & 300 & 0 \\
0 & 0 & 0 & 0 \\
0 & 0 & 0 & 300
\end{bmatrix}
$$

APPENDIX B
FULL-STATE FEEDBACK GAIN MATRICES

Longitudinal Gains

Columns 1 through 7

$$K = \begin{matrix} & q & \alpha & V & \theta & & & \\ \ulcorner & & & & & & & \\ & 0.5938 & -0.4672 & 0.0026 & 0.7803 & -0.0000 & 0.0000 & 0.0000 \\ & 1.7524 & -1.2850 & 0.0021 & 2.3451 & -0.0000 & 0.0000 & 0.0000 \\ & 1.7524 & -1.2850 & 0.0021 & 2.3451 & -0.0000 & 0.0000 & 0.0000 \\ \llcorner & 0.5938 & -0.4672 & 0.0026 & 0.7803 & -0.0000 & 0.0000 & 0.0000 \end{matrix}$$

Columns 8 through 13

$$\begin{matrix} 0.0000 & 0.0000 & 0.0000 & 0.0000 & 0.0000 & 0.0000 \\ 0.0000 & 0.0000 & 0.0000 & 0.0000 & 0.0000 & 0.0000 \\ 0.0000 & 0.0000 & 0.0000 & 0.0000 & 0.0000 & 0.0000 \\ 0.0000 & 0.0000 & 0.0000 & 0.0000 & 0.0000 & 0.0000 \end{matrix} \times 10^3$$

Lateral-Directional Gains

Columns 1 through 7

$$K = \begin{matrix} & P & r & \beta & \phi & & & \\ \ulcorner & & & & & & & \\ & 93.9147 & 583.5935 & 91.5507 & 124.5400 & 0.0000 & 0.0092 & 0.0056 \\ & 55.3452 & 343.9231 & 53.9600 & 73.3935 & 0.0000 & 0.0032 & 0.0013 \\ & -55.3452 & -343.9231 & -53.9600 & -73.3935 & -0.0000 & -0.0032 & -0.0013 \\ \llcorner & -93.9147 & -583.5935 & -91.5507 & -124.5400 & -0.0000 & -0.0054 & -0.0022 \end{matrix}$$

Columns 8 through 13

$$\begin{matrix} 0.0032 & 0.0013 & -0.0032 & -0.0013 & -0.0054 & -0.0022 \\ 0.0057 & 0.0041 & -0.0019 & -0.0008 & -0.0032 & -0.0013 \\ -0.0019 & -0.0008 & 0.0057 & 0.0041 & 0.0032 & 0.0013 \\ -0.0032 & -0.0013 & 0.0032 & 0.0013 & 0.0092 & 0.0056 \end{matrix}$$

APPENDIX C
MOVEMENT OF ROOTS WITH LONGITUDINAL, LATERAL, AND COMBINED REGULATION

Open loop	Longitudinal regulator	Lateral-directional regulator	Combined longitudinal and lateral-directional regulator
1.0000	1.0000	1.0000	1.0000
0.5773 + 0.3112i	0.7725 + 0.3176i	0.5773 + 0.3112i	0.7725 + 0.3176i
0.5773 – 0.3112i	0.7725 – 0.3176i	0.5773 – 0.3112i	0.7725 – 0.3176i
0.9971 + 0.0586i	0.6198 + 0.3245i	0.9971 + 0.0586i	0.6198 + 0.3245i
0.9971 – 0.0586i	0.6198 – 0.3245i	0.9971 – 0.0586i	0.6198 – 0.3245i
1.0003	0.4000	1.0003	0.9999
0.8090 + 0.4797i	0.5216 + 0.2243i	0.7266 + 0.5125i	0.9688
0.8090 – 0.4797i	0.5216 – 0.2243i	0.7266 – 0.5125i	0.4000
0.5898	0.9688	0.9049 + 0.3484i	0.5216 + 0.2243i
0.9986	0.9999	0.9049 – 0.3484i	0.5216 – 0.2243i
0.5173 + 0.2325i	0.8090 + 0.4797i	0.3655	0.7266 + 0.5125i
0.5173 – 0.2325i	0.8090 – 0.4797i	0.5899	0.7266 – 0.5125i
0.5173 + 0.2325i	0.9986	0.5173 + 0.2325i	0.9049 + 0.3484i
0.5173 – 0.2325i	0.5898	0.5173 – 0.2325i	0.9049 – 0.3484i
0.5173 + 0.2325i	0.5173 + 0.2325i	0.5173 + 0.2325i	0.3655
0.5173 – 0.2325i	0.5173 – 0.2325i	0.5173 – 0.2325i	0.5173 + 0.2325i
0.5173 + 0.2325i	0.5173 + 0.2325i	0.5173 + 0.2325i	0.5173 + 0.2325i
0.5173 – 0.2325i	0.5173 – 0.2325i	0.5173 – 0.2325i	0.5899

APPENDIX D
EVALUATION OF FIRST LATERAL-DIRECTIONAL DESIGN

The original design evaluation for lateral-directional gains through linear simulation are shown in figures D-1 to D-6.

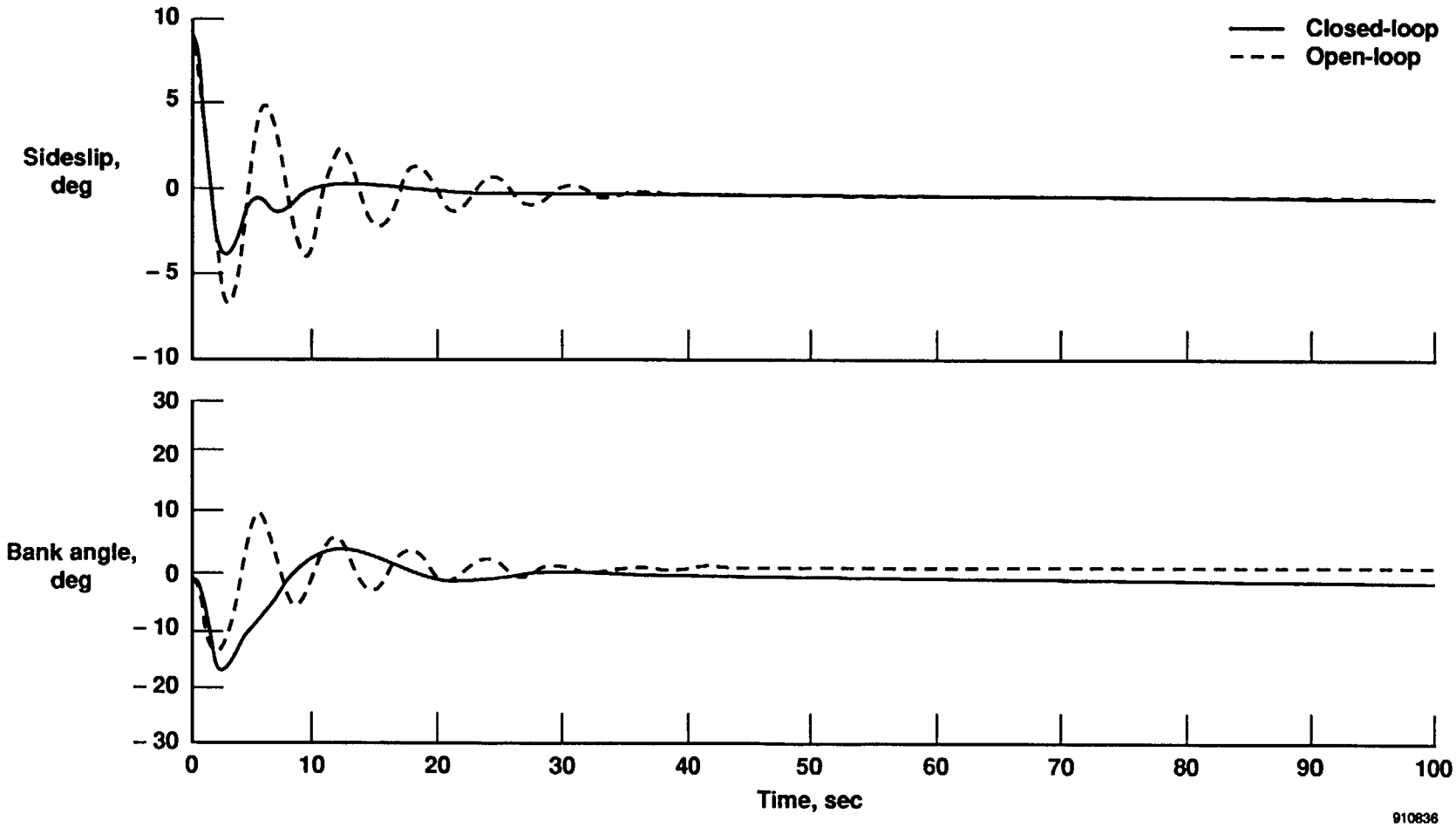

Figure D-1. Bank angle and sideslip response to an initial condition of q = 10 deg/sec, $\alpha = 5°$, and $\beta = 10°$.

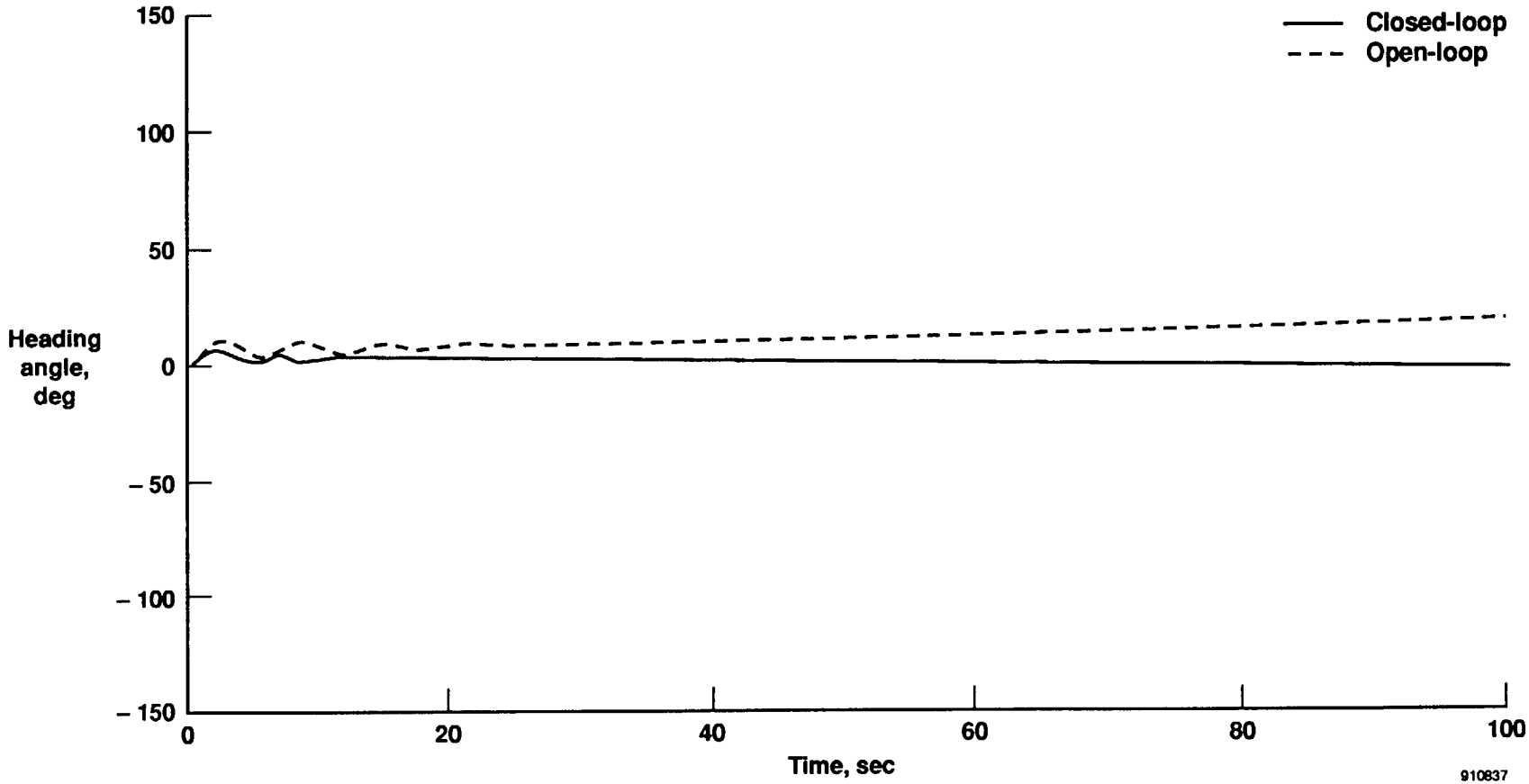

Figure D-2. Heading angle response to an initial condition of q = 10 deg/sec, $\alpha = 5°$, and $\beta = 10°$.

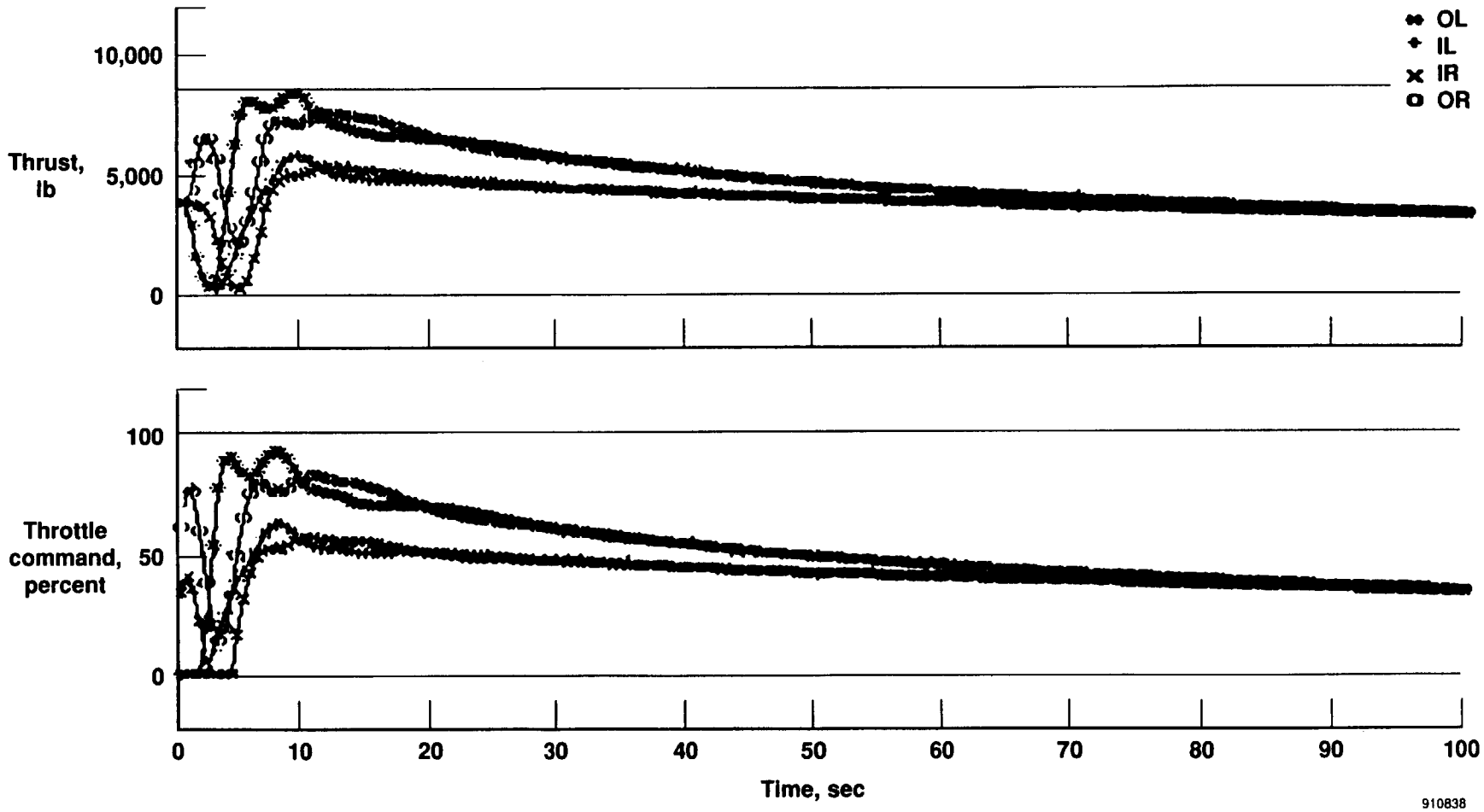

Figure D-3. Throttle command and thrust response to an initial condition of q = 10 deg/sec, $\alpha = 5°$, and $\beta = 10°$.

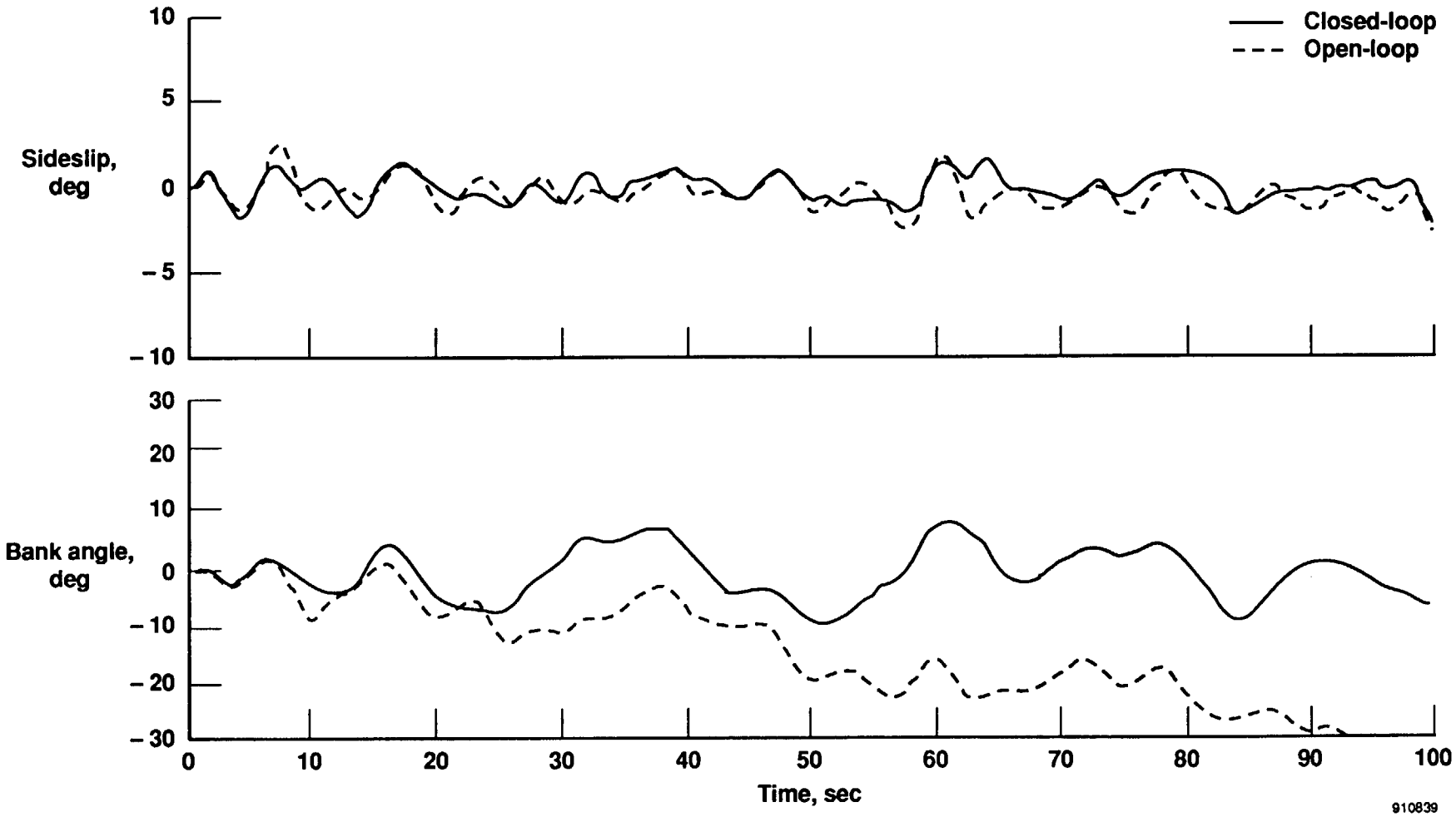

Figure D-4. Bank angle and sideslip response to random excitation, $3\sigma = \{2\ 1\ 5\ 1\ 5\ 2\ 2\ 1\ 1\ 1\}$.

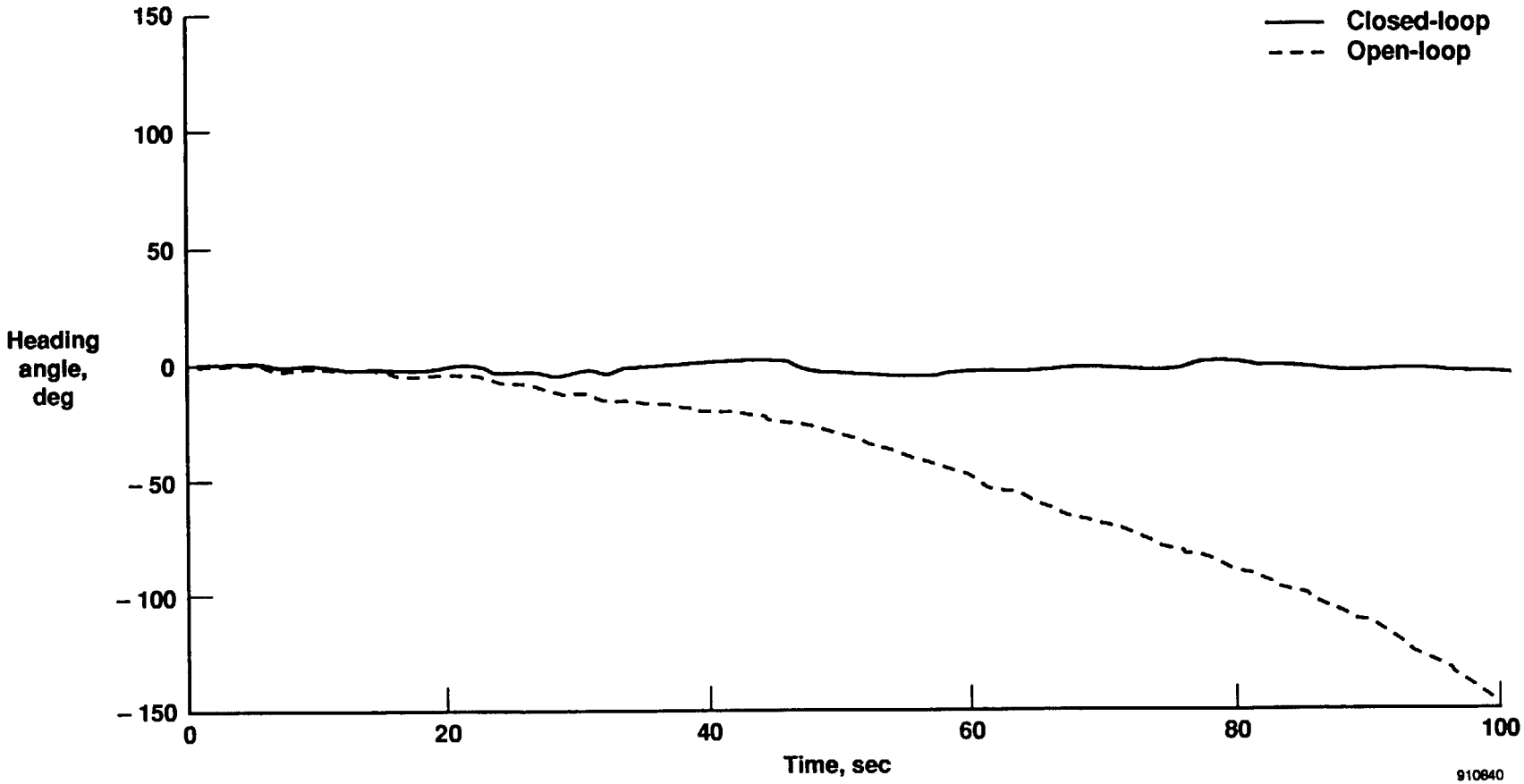

Figure D-5. Heading angle response to random excitation, $3\sigma = \{2\ 1\ 5\ 1\ 5\ 2\ 2\ 1\ 1\ 1\}$.

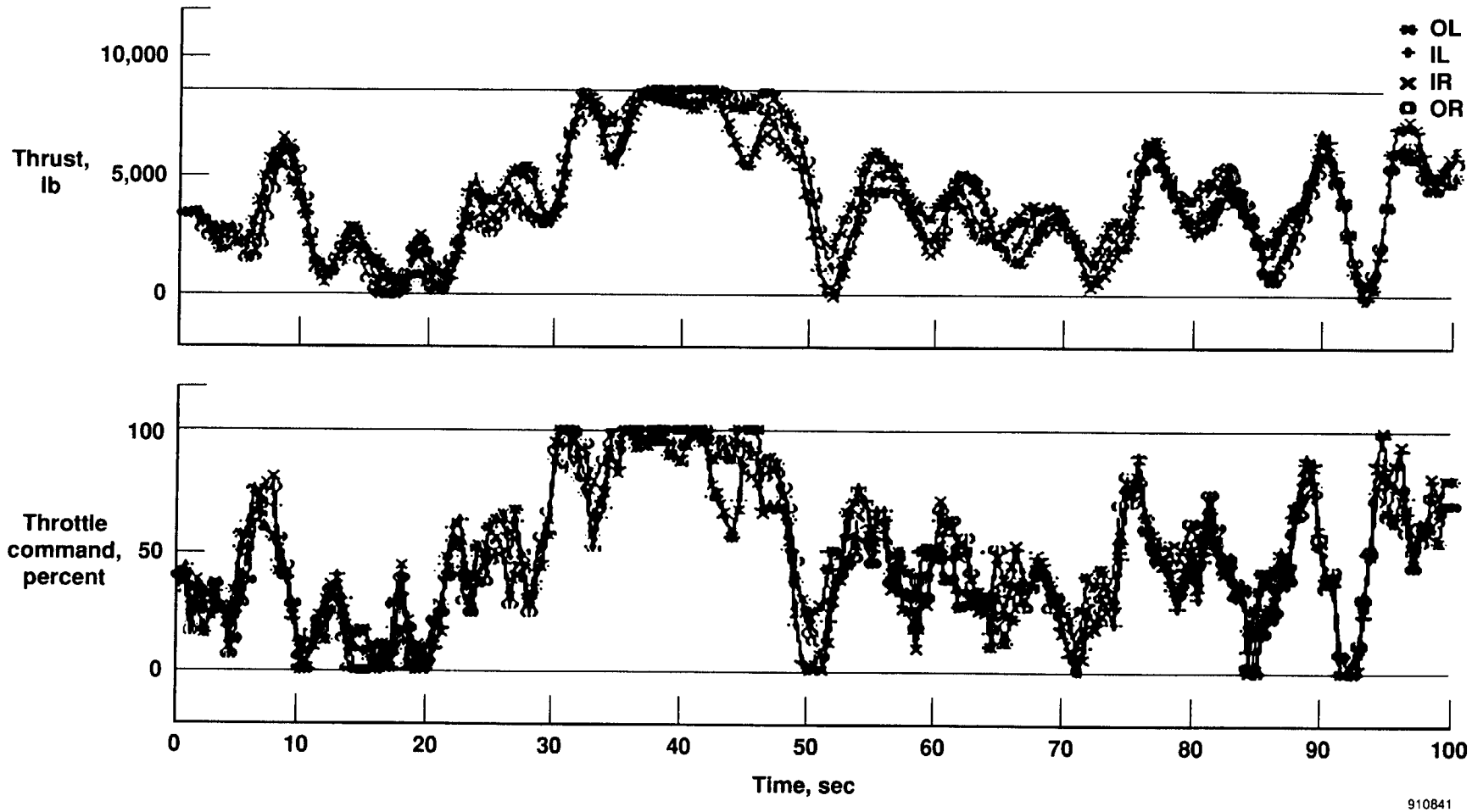

Figure D-6. Throttle command and thrust response to random excitation, $3\sigma = \{2\ 1\ 5\ 1\ 5\ 2\ 2\ 1\ 1\ 1\}$.

REPORT DOCUMENTATION PAGE

Form Approved
OMB No. 0704-0188

1. AGENCY USE ONLY *(Leave blank)*	2. REPORT DATE	3. REPORT TYPE AND DATES COVERED
	April 1992	Contractor Report - Final

4. TITLE AND SUBTITLE

A Preliminary Look at an Optimal Multivariable Design for Propulsion-Only Flight Control of Jet-Transport Aircraft

5. FUNDING NUMBERS

RTOP 533-02-21

6. AUTHOR(S)

Christopher P. Azzano

7. PERFORMING ORGANIZATION NAME(S) AND ADDRESS(ES)

NASA Dryden Flight Research Facility
P.O. Box 273
Edwards, California 93523-0273

8. PERFORMING ORGANIZATION REPORT NUMBER

H-1729

9. SPONSORING/MONITORING AGENCY NAME(S) AND ADDRESS(ES)

National Aeronautics and Space Administration
Washington, DC 20546-0001

10. SPONSORING/MONITORING AGENCY REPORT NUMBER

NASA CR-186014

11. SUPPLEMENTARY NOTES

This report was prepared during an intern program. NASA Technical Monitor: Glenn Gilyard, Dryden Flight Research Facility, Edwards, CA 93523.

12a. DISTRIBUTION/AVAILABILITY STATEMENT

Unclassified — Unlimited
Subject Category 08

12b. DISTRIBUTION CODE

13. ABSTRACT ***(Maximum 200 words)***

Control of a large jet-transport aircraft without the use of conventional control surfaces was investigated. Engine commands were used to attempt to recreate the forces and moments typically provided by the elevator, ailerons, and rudder. Necessary conditions for aircraft controllability (disturbability) were developed pertaining to aircraft configuration such as the number of engines and engine placement. An optimal linear quadratic regulator controller was developed for the Boeing 707-720, in particular, for regulation of its natural dynamic modes. The design employed a method of assigning relative weights to the natural modes, for example, phugoid and dutch roll, for a more intuitive selection of the cost function. A prototype pilot command interface was then integrated into the loop based on pseudorate command of both pitch and roll. Closed-loop dynamics were evaluated first with a batch linear simulation and then with a real-time high fidelity piloted simulation. The NASA research pilots assisted in evaluation of closed-loop handling qualities for typical cruise and landing tasks. Recommendations for improvement on this preliminary study of optimal propulsion-only flight control are provided in the report.

14. SUBJECT TERMS	15. NUMBER OF PAGES
Aircraft and engine modeling; Aircraft handling qualities; Flight control systems; Modal regulator design; Propulsion-enhanced flight control	55
	16. PRICE CODE: A04

17. SECURITY CLASSIFICATION OF REPORT	18. SECURITY CLASSIFICATION OF THIS PAGE	19. SECURITY CLASSIFICATION OF ABSTRACT	20. LIMITATION OF ABSTRACT
Unclassified	Unclassified	Unclassified	Unlimited